

Carbon soil stock change in an intensive crop field near Paris reveals significant carbon losses over a decade

Benjamin Loubet^{1*}, Nicolas P.A. Saby², Bruna Winck^{1,2}, Maryam Gebleh^{1,2}, Pauline Buysse^{1,3}, Jean-Philippe Chenu², Céline Ratié², Claudy Jolivet², Carmen Kalalian¹, Florent Levavasseur¹, Jose-Luis Munera-Echeverri², Sébastien Lafont⁴, Denis Loustau⁴, Dario Papale^{5,6}, Giacomo Nicolini⁷, and Dominique Arrouays^{2 †}

1 ECOSYS, University Paris-Saclay, INRAE, AgroParisTech, Palaiseau, France

2 Info&Sols, INRAE, Orléans, France

3 SAS, INRAE, Institut Agro Rennes-Angers, Rennes, France

4 Bordeaux Sciences-Agro, INRAE, ISPA, F-33610, Villenave d'Ornon, France

5 CNR IRET, Monterotondo Scalo, Italy

6 University of Tuscia, DIBAF, Viterbo, Italy

7 CMCC Foundation - Euro-Mediterranean Center on Climate Change, Viterbo, Italy

† deceased

* corresponding author: benjamin.loubet@inrae.fr

Abstract. Soil is a large pool of carbon (C), storing globally twice and three times more carbon than the atmosphere and vegetation, respectively. Soil organic carbon (SOC) stocks are significantly impacted by land use changes, either negatively when forest or grasslands are turned into crops or positively when the opposite is done. This context underpins the “4per1000” initiative, which aims to promote SOC storage in soils as a mitigation strategy. However, intensive cropping and climate change may lead to organic and inorganic carbon losses from soils, which calls for long-term observations of soil organic carbon stocks in reference ecosystems over the globe. To address this, a harmonised reference soil sampling protocol was developed for all ecosystem sites within the European Integrated Carbon Observing System (ICOS) research infrastructure, starting in 2017 with revisits planned every 5–10 years. This study presents a first case at the French cropland site FR-Gri (wheat–maize–barley–oilseed rape rotation), assessing SOC stock in 2019 with the ICOS protocol, which was combined with earlier SOC stock sampling data from the European project CarboEurope. A significant soil decompaction was observed over the 13.5 years up to 30 cm. Bulk density decreased by 22% in the 0-5 cm layer (from 1.31 to 1.02 g cm⁻³) and by 5% in the 5-30 cm layer (from 1.53 to 1.45 g cm⁻³), likely due to the adoption of reduced tillage since 2004. SOC content increased by 10% in the 0-5 cm layer, but declined in the 5-30 cm layer by 6.2%. The SOC stocks based on equivalent soil mass (ESM) increased by 7.6% in the 0-5 cm layer, but decreased by 11% and 9% in the 5-30 and 30-60 cm layers. Overall, the ESM-based cumulative SOC stock in the 0-60 cm layer decreased by approximately 0.95 ± 0.22 kg C m⁻² (or 9 Mg C ha⁻¹) between 2005 and 2019, corresponding to an average decrease rate of 0.072 ± 0.017 kg C m⁻² yr⁻¹ (or 0.72 ± 0.17 Mg C ha⁻¹) or 0.65% year⁻¹, consistent with previous studies. To further interpret this trend, we applied the soil carbon cycling model AMG to simulate SOC dynamics down to 30 cm depth from 2005 onwards. Based on site-specific exports and imports and estimated residue returns, the model predicted a continuous SOC stock decline under current management, stabilising around 2028. The SOC stock decrease aligns with the changes observed between 2005 and 2019 over the whole soil profile, but is larger than the stock change over the 0-30 cm depth. By 2040, SOC stocks are projected to decline to 6.9 kg C m⁻², representing an approximate 15% reduction from the 2005 baseline. Furthermore, the AMG simulation was also consistent with the carbon flux balance reported between 2006 and 2010 by Loubet et al. (2011). This observed SOC stocks

decrease may be explained by a shift towards larger exportations and lower residue returns at this site compared to past management practices. This underscores the need for high-quality SOC stock change monitoring, as developed by the ICOS research infrastructure, to provide clearer insights into this important challenge.

1 Introduction

45 Soil is a significant carbon (C) and nitrogen (N) biogeochemical cycle pool. According to the latest estimations, soils store 1500 to 2400 Gt C globally to a depth of 1 m as organic matter (Batjes, 1996; Sanderman et al., 2017) and almost the same amount as inorganic C to a depth of 2 m (Zamanian et al., 2021). Soils contain approximately twice as much organic C as the atmosphere and vegetation (Antón et al., 2021). Hence, minor changes in this large soil reservoir could affect future atmospheric carbon dioxide (CO₂) concentrations (Minasny et al., 2017). Soil
50 organic carbon (SOC) stocks are significantly impacted by land use through crop and forest management. It is estimated that soils have globally lost 140 to 150 Gt of organic carbon due to land use intensification since the onset of agriculture 8000 to 120000 years ago (Sanderman et al., 2017; Schimel, 1995). Likewise, increased N deposition and intensification of N use in agriculture since the 20th century have also affected soil inorganic carbon (SIC) stocks, reducing them through carbonate weathering. This process, together with global warming, could
55 counteract efforts to increase SOC by changing land management (Raza et al., 2020; Schrumpf et al., 2011; Song et al., 2022; Zamanian et al., 2021).

The impact of agricultural management on SOC stocks depends on the interaction between management practices, climate, and soil type (Paustian et al., 2016). Intensive farming in the 20th century, characterised by monoculture, soil tillage, and high fertiliser use, has aggravated climate change (Autret et al., 2016), notably through increased
60 nitrous oxide (N₂O) emissions, which accounted for 74% of the total anthropogenic N₂O emissions in the last decade (Tian et al., 2024). Beyond N₂O, these practices also contribute to CO₂ emissions, primarily by releasing protected soil carbon into the atmosphere (Autret et al., 2016; Schmidt et al., 2011; Six et al., 2002). However, recent studies have shown that N fertilisation (Skadell et al., 2023) and occasional deep tillage can enhance SOC stocks by incorporating organic matter into deep layers (Krauss et al., 2022). Evidence also support the adoption
65 of conservation agricultural practices, such as cover crop, high organic inputs, and diverse crop rotations, to restore SOC and mitigate climate change by enhancing C inputs and persistence in soil (Lal, 2004; Poeplau and Don, 2015, Schmidt et al., 2011), despite some carbon losses due to priming effects (Chen et al., 2019). Minimum and no-tillage have been promoted to increase SOC stocks, with a postulated sequestration of 2 to 3 Pg C yr⁻¹ in the top meter of agricultural soils by increasing carbon stocks by 4 per 1000 annually. If achieved, this level of se-
70 questration could offset approximately one-third of global anthropogenic greenhouse gas emissions (Minasny et al., 2017). However, these estimates may be overly optimistic, as C sequestration declines over time while the soil approaches a new equilibrium (Baveye et al., 2018; Franzluebbers et al., 2012). Moreover, growing evidence shows that their effectiveness may be limited unless they are combined with other conservation practices (Chenu et al., 2019). For instance, in France, Meersmans et al. (2016) suggested that significant SOC gains are only possible through the conversion of cropland to forest or grasslands, although expanding conservation practices and
75 integrating temporary grasslands into crop rotations can also contribute meaningfully to SOC gains at the national scale (Launay et al., 2021). Although the primary objective today is climate mitigation through enhanced carbon stocks and diminished GHG emissions, including CO₂, N₂O and CH₄, it is crucial that strategies designed to

80 achieve this goal are balanced with other priorities, including ensuring global food security and minimising environmental impacts.

Overall, nowadays, European croplands are considered a net carbon source to the atmosphere of $10 \pm 9 \text{ g C m}^{-2} \text{ yr}^{-1}$, while grasslands and forests are net atmospheric sinks of $57 \pm 34 \text{ g C m}^{-2} \text{ yr}^{-1}$ and $20 \pm 12 \text{ g C m}^{-2} \text{ yr}^{-1}$ (Schrumpf et al., 2011; Schulze et al., 2009). A recent review of bottom-up estimates and national inventories in Europe finds that terrestrial ecosystems are an overall sink of $\sim -100 \text{ Tg C yr}^{-1}$, an estimate that is characterised by large uncertainties of $\pm 360 \text{ Tg C yr}^{-1}$ (Petrescu et al., 2021). The same review shows that top-down estimates are affected by an even higher uncertainty, too large to allow for the verification of national inventories. Therefore, accurately determining SOC stocks and their changes with time is essential to verify the actual carbon fluxes to ecosystems and monitor their evolution over time (Poeplau et al., 2017).

90 The monitoring of SOC stocks is subject to uncertainties, making it challenging to detect and accurately quantify their changes reliably. Indeed, accurate monitoring of SOC stocks needs quantification of both the mass and the organic carbon (OC) content of the soil fine earth fraction ($< 2 \text{ mm}$) across the soil layers (Molteni and Corti, 1998). These soil properties are highly variable spatially and require dense sampling to reduce the uncertainty and be able to detect SOC changes over time (Batjes, 1996). Moreover, the rock fraction (RF), evaluated as the coarse mineral fragments larger than 2 mm , is assumed to be free of organic matter, which is only partially accurate (Corti et al., 1998). Measuring soil fine earth fraction relies on bulk density (BD) and RF measurements, which are time-consuming. Bulk density is often estimated by pedo-transfer functions (PTF), which are known to produce random errors and are prone to systematic biases (Harbo et al., 2022; Knotters et al., 2022; Schrumpf et al., 2011). In some studies, the choices of PTF equations, along with the neglect of RF, lead to systematic uncertainties in SOC stock estimates, among which RF is the most critical (Beem-Miller et al., 2016; Poeplau et al., 2017; Wiesmeier et al., 2012). Likewise, many PTFs use SOC content as an input variable to predict BD, which is subsequently used to estimate SOC stocks. This interdependence introduces a potential circularity in the estimation process. If the uncertainty associated with the PTF is not properly accounted for, this dependency can introduce systematic bias and increase the variance and overall uncertainty of SOC stock estimates (Schrumpf et al., 2011; Xu et al., 2015).

105 Changes in BD over time need to be considered when monitoring SOC stock changes over the decades. Indeed, significant BD variation may result from intense swelling and shrinkage in clayey soil (particularly in expandable clay soils) driven by climate change and seasonality, compaction and decompaction linked to agricultural practices and water content, and erosion (Hopkins et al., 2009). To address this issue, Ellert and Bettany (1995) proposed the equivalent soil mass (ESM) method instead of the fixed depth (FD) method to measure SOC stock changes. In the FD method, SOC stock changes over time are evaluated at constant soil depths and can induce significant biases due to the variation in BD (Beem-Miller et al., 2016). In the ESM approach, SOC stocks are evaluated for a constant soil mass per unit area, thereby compensating for changes in BD by adjusting the soil depth accordingly (Ellert and Bettany, 1995; von Haden et al., 2020; VandenBygaart and Angers, 2006; Wendt and Hauser, 2013). Differences between FD and ESM can overwhelm variations caused by tillage and crop residue removal rates in the range of 10% of SOC changes (Du et al., 2017; Xiao et al., 2020). As comparing SOC stocks on the same soil mass per unit area is recognised as a better practice than the FD approach, this methodology was included as the reference method by FAO and IPCC (FAO, 2019; IPCC, 2019).

115 Soil organic carbon stocks are key evaluations that are included in the ICOS (Integrated Carbon Observation System) European Research Infrastructure Consortium (Heiskanen et al., 2022). As of 2025, ICOS included 45 high-

120 quality and standardised ecosystem sites (Class 1 and 2 stations), covering the diversity of European soils and
ecosystems. At each site, the SOC stock is measured when the site enters ICOS and from 5 to 10 years later to
evaluate the SOC stock change over time. This change can then be compared to the integrated carbon fluxes at the
site boundaries over that period, which comprise the net ecosystem productivity, imports to and exports from the
site, and lixiviated fluxes (Aubinet et al., 2009; Ceschia et al., 2010; Loubet et al., 2011). Soil carbon cycling
models such as DAYCENT (Parton et al., 1998), Stics (Brisson et al., 1998), RothC (Coleman and Jenkinson,
125 1996) or AMG (Clivot et al., 2019) are essential tools to further understand the observed SOC dynamics based on
site-specific managements, and in particular exports, imports and residue returns. Models are also key in providing
long-term simulation of SOC stock dynamics and scenario analysis.

Monitoring SOC stocks also requires an adequate sampling strategy that ensures unbiased and robust estimates
with a limited number of samples (Arrouays et al., 2018; Don et al., 2007; Saby et al., 2008). Within the ICOS
130 network, soils started to be sampled in 2017, adopting a Design-Based (DB) approach (Brown, 1992; Collins,
1992). This method relies on randomly chosen sampling points, which increases the precision of the mean or total
estimates (Arrouays et al., 2018; Brus and deGrujter, 1997; de Grujter et al., 2006; Loustau et al., 2017). About
half of the sites have been sampled in 2025, and given a 10-year interval time, the first SOC stock change evalua-
tions at these sites with the ICOS methodology will only be available from 2027 onward.

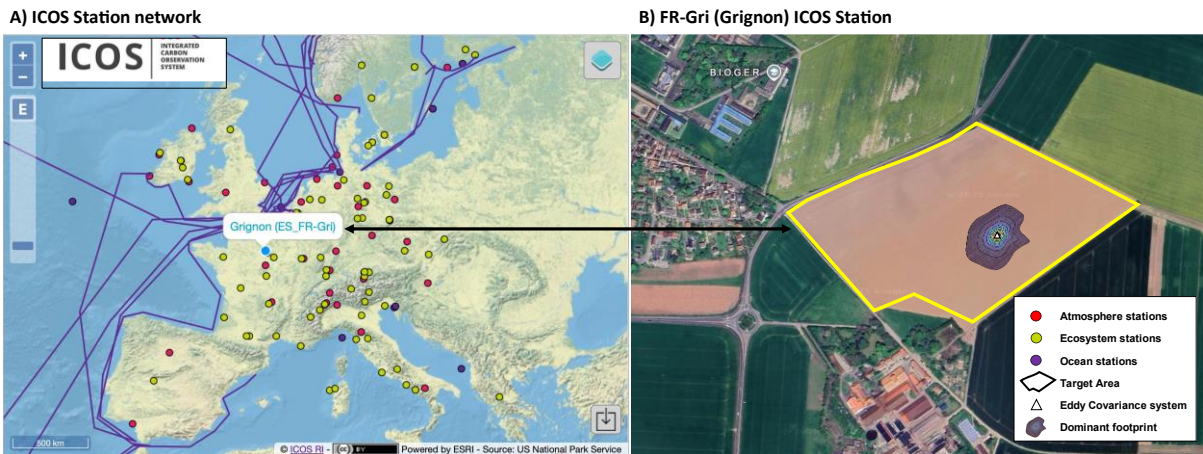
135 However, 12 ICOS sites were sampled from 2005 to 2010 using a systematic grid-based sampling approach within
the EU CarboEurope project, as reported by Schrumpf et al. (2011). At the Grignon station (ICOS code FR-Gri),
a cropland site SOC was measured in 2005 using the grid-based design and again in 2019 using the ICOS protocol.
This raises the question of whether these earlier data can be reliably leveraged to assess SOC stock changes over
the past 14 years.

140 The main objectives of this study are to (1) evaluate the SOC stock change between 2005 and 2019 at FR-Gri
station, (2) compare the equivalent soil mass and fixed depth SOC stock changes calculations, and (3) discuss the
uncertainties in these estimations, and (4) compare the results to the soil carbon cycle model AMG prediction
(Clivot et al., 2019) and to previously established carbon flux balance estimations at the same site by Loubet et al.
(2011).

145 2 Materials and methods

2.1 Study site

The study was conducted at the Grignon station, an ICOS ecosystem site (ICOS code FR-Gri, class 2 since 2021).
It is a crop field of 19 ha located 40 km west of Paris, in northern France (48.9°N, 1.95°E; elevation 125 m) (**Figure
1**). During the studied years (between 2005 and 2019), the mean annual air temperature and rainfall were 11.2 °C
150 and 586 mm, respectively. The site has a gentle north-eastward slope of approximately 1%. Agricultural fields
mostly surround the south and west of the study area. The surface soil (0–15 cm layer) is classified as silt loam,
with a particle-size distribution of 98 g kg⁻¹ sand, 713 g kg⁻¹ silt, and 189 g kg⁻¹ clay. The effective soil depth (A
+ B horizons) varies from approximately 0.4 m in the north-east to over 1 m in the south-west. Soils across the
parcel exhibit calcic horizons, with average CaCO₃ contents of 3% in the 0–50 cm layer and 20% in the 50–100
155 cm layer and an alkaline soil pH of 7.6. (**Table S1**). The OC content in the surface layers was around 20 g C kg⁻¹,
as reported in 2011 (Loubet et al., 2011).



160 **Figure 1. (A) Map of the ICOS station network across Europe, showing atmosphere (red), ecosystem (green), and ocean**
(blue) stations. The Grignon site (FR-Gri) is highlighted. (B) The 19-ha field site at FR-Gri, shown in a Google Maps
image, with the target area outlined in yellow. The eddy covariance system (white triangle) is located centrally, sur-
rounded by its dominant flux footprint (shaded gradient area). The site, with a mixed farm with cattle and sheep housed
highly fertilised with sewage sludge in the 1980s. On the left, the image is taken from the ICOS web site © ICOS RI. On
165 **the right the image was taken from the French GeoPortal © IGN 2023. The image was taken in 2021.**

In 2004, as part of the implementation of reduced tillage and the crop rotation system, the soil was scarified to a depth of 50 cm to reduce compaction. Since then, most tillage operations have been restricted to the superficial layer (0–15 cm), using a stubble cultivator or clod crusher. Two additional scarification events were carried out:
170 one in 2010 (to a depth of 25 cm) and another in 2012 (to a depth of 40 cm). Additionally, the soil is disturbed to a depth of 5 or 10 cm during seeding operations.

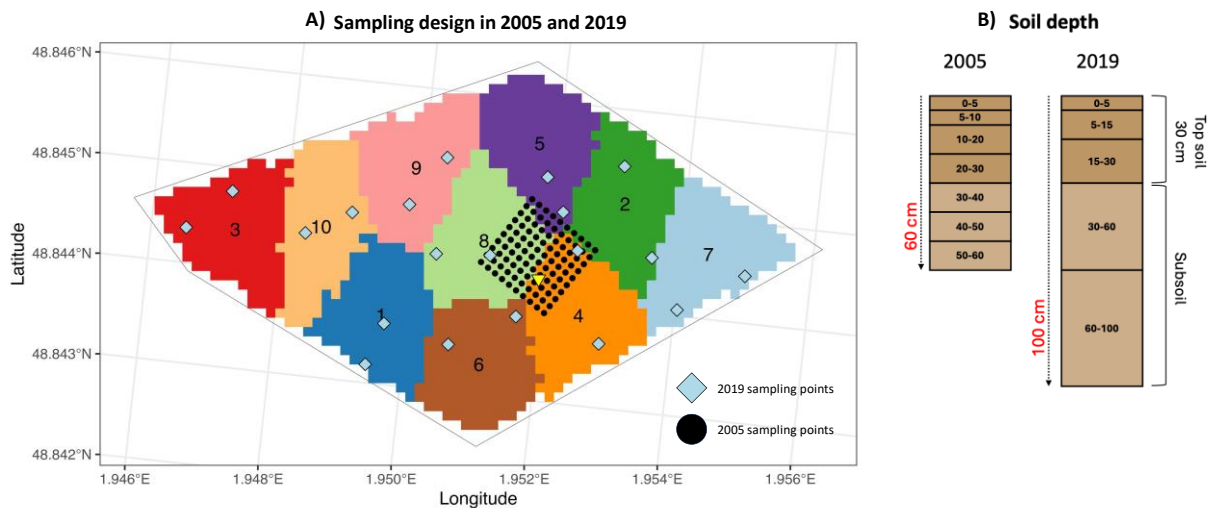
Table 1. Crop rotation, yield, exports and imports, and nitrogen (N) applied over the 15 years between the two sampling campaigns at the FR-Gri site. Carbon export was evaluated based on the farmer's record of grain, straw and silage exports. The aerial crop residue return was evaluated based on the exports and the allometric coefficient of the AMG model, as explained in the manuscript. A 0.44 g C g⁻¹ dry biomass carbon content was assumed to compute the exports and imports. Organic nitrogen was mainly cattle slurry and, on a few occasions, manure. Mineral fertilisation was mainly urea, ammonium nitrate.

crop	year	part of the plant harvested	Exported Carbon (g C m ⁻²)	Imported Carbon (g C m ⁻²)	Aerial Crop Residues returned to the soil (g C m ⁻²)	Organic Nitrogen applied (kg N ha ⁻¹)	Mineral Nitrogen applied (kg N ha ⁻¹)	Total Nitrogen applied (kg N ha ⁻¹)
mustard	2005	None			90 ± 10			
maize	2005	above 20 cm -	330 ± 40		10 ± 0		140 ± 10	140 ± 10
wheat	2006	seed and straw	640 ± 70		170 ± 20		110 ± 10	110 ± 10
barley	2007	seed and straw	440 ± 50		150 ± 20		110 ± 10	110 ± 10
mustard	2008	None			90 ± 10			
maize	2008	above 20 cm -	550 ± 60	120 ± 20	20 ± 0	80 ± 10	60 ± 0	130 ± 10
wheat	2009	seed, straw and chaff	640 ± 70	140 ± 20	150 ± 10	80 ± 10	170 ± 10	250 ± 20
Triticale	2010	seed, straw and chaff	490 ± 60	240 ± 40	90 ± 10	220 ± 40	100 ± 10	320 ± 40
maize	2011	above 20 cm -	610 ± 70	120 ± 20	20 ± 0	80 ± 10		80 ± 10
wheat	2012	seed, straw and chaff	640 ± 70	160 ± 30	100 ± 10	170 ± 30	70 ± 0	240 ± 30
rapeseed	2013	seed and chaff	240 ± 30		370 ± 40		110 ± 10	110 ± 10
wheat	2014	seed and straw	420 ± 50	180 ± 30	110 ± 10	130 ± 20	110 ± 10	240 ± 20
mustard	2015	None			90 ± 10			
maize	2015	above 20 cm -	430 ± 50	280 ± 50	20 ± 0	290 ± 50		290 ± 50
wheat	2016	seed, straw and chaff	440 ± 50	50 ± 10	190 ± 20	90 ± 20	220 ± 10	310 ± 20
rapeseed	2017	seed	170 ± 20		440 ± 40	0 ± 0	120 ± 10	120 ± 10
wheat	2018	seed and straw	450 ± 50	300 ± 50	130 ± 10	190 ± 30	80 ± 0	270 ± 30
mix intercrop	2019	All plants for silage	50 ± 10				40 ± 0	40 ± 0
maize	2019	above 20 cm -	540 ± 60	120 ± 20	20 ± 0	80 ± 10		150 ± 10
		average (g C m ⁻² y ⁻¹ or kg N ha ⁻¹)	470 ± 54	114 ± 13	151 ± 17	93 ± 11	100 ± 11	193 ± 22

The crops in the rotation system are winter wheat, silage maize (preceded by a mustard catch crop), and winter barley, with two years of oilseed rape during the period (**Table 1**). These crops are herbaceous, mixing C3 (wheat, barley, triticale, oilseed rape, mustard) and C4 (maize) plants. The crop production is mainly exported as grain or silage (maize), but residues are also exported for animals and bioenergy. The average carbon export was 470 ± 54 g C m⁻² yr⁻¹ (**Table 1**). The field received some slurry and manure regularly, with an average carbon input of 114 ± 13 g C m⁻² yr⁻¹. The average above-ground biomass crop residues left on the field were evaluated using the exported biomass and allometric coefficients (Clivot et al., 2019). They represent 151 ± 17 g C m⁻² yr⁻¹, around 1/3 of the exported carbon, slightly higher than the imported one. The biomass of mustard was not measured but taken equal to the mean estimated biomass of mustard in France – 2 Mg DM ha⁻¹ (Soleilhavoup and Crisan, 2021).

2.2 Soil sampling schemes

The two campaigns were carried out in different areas around the eddy covariance system: the 2005 campaign focused on an area representative of the eddy-covariance mast maximum footprint, while the 2019 campaign encompassed the whole 19 ha field. The footprint determined using the Kljun approach (Kljun et al., 2004, 2015), was well inside the 19-ha field (**Figure 1**) except for some stable nights when it reached the surroundings. Two different soil sampling strategies were used during the two campaigns in 2005 and 2019 (**Figure 2**). In the 2005 campaign, 100 soil cores were taken following a systematic random sampling corresponding to a regular grid (7 × 7 m), and samples were collected using both 8.3 and 8.7 cm inner diameter corers in December 2005 during winter wheat dormancy. Soil cores were divided into seven layers (0-5, 5-10, 10-20, 20-30, 30-40, 40-50, and 50-60 cm). The 2005 campaign results were reported in Schruppf et al. (2011). In the 2019 campaign, 99 soil samples (20 locations × 5 depths – 1) were collected in March, following the ICOS protocol (Arrouays et al., 2018; Loustau et al., 2017), which consists of a stratified simple random sampling design. One sample between 60 and 100 cm was not reachable due to rock density. The field was at that time covered with a mix of catch crops (oats, field bean, pea, clover, and flax). The studied area was divided into 10 geographically compact equal-area strata (Walvoort et al., 2010). Within each stratum, two primary sampling points (SP-I) were randomly selected (simple random) for a total of 20 SP-I plots. At each SP-I, five secondary sampling points (SP-II) were randomly selected within a buffer area of 10 meters, where the soil was sampled using a 5.5 cm inner diameter corer. Each core was separated into sub-samples at 0-5, 5-15, 15-30, 30-60 and 60-100 cm depth. Finally, cores were mixed to form a composite sample at each primary location and each layer. The spatial stratification and sampling point distribution were performed using the R package “*spsosa*” (Walvoort et al., 2010).



210

Figure 2. A) Map of the study area showing the spatial distribution of sampling zones and soil core depth segmentation. Soil sampling was conducted at two times: in 2005 (black circles) and 2019 (blue diamonds). For the 2019 sampling, the field was stratified into 10 strata (coloured polygons, labelled 1–10), and the sampling points were randomly located within each stratum. The 2005 sampling followed a grid-based sampling design partially covering strata 2, 4, 5 and 8, and mostly concentrated in strata 8 and 4. B) Segmentation of soil cores into depth intervals for two different sampling protocols: 60 cm cores (six layers: 0–5, 5–10, 10–20, 20–30, 30–40, and 50–60 cm) and 100 cm cores (five layers: 0–5, 5–15, 15–30, 30–60, and 60–100 cm). Latitude and longitude are shown in WGS 84 coordinates.

215

2.3 Soil samples preparation and analyses

220

In the 2005 campaign, all soil samples were preserved at 4°C before processing. The coarse fraction – rock (RF) ($\varnothing > 4$ mm) and root fractions ($\varnothing > 1$ mm) - were separated from the samples and subsequently air-dried at 40°C. The remaining samples were sieved to < 2 mm to obtain the fine earth (FE) fraction and the coarse fraction (> 2 mm). Subsequently, each fraction was weighted (Schrumpp et al., 2011). In the 2019 campaign, the samples from SP-II plots were air-dried at 30°C and then sieved to separate the FE fraction (< 2 mm), and the root and rock fractions were oven-dried at 70°C and 105°C, respectively, before weighing. Subsequently, the FE fraction from each depth interval of the five SP-II plots was proportionally mixed (based on the weight contribution of each layer) to create a composite sample (SP-I). The BD, residual water and FE fraction were computed from the SP-II samples, then averaged at the SP-I level, and the C content was measured on the SP-I composite samples. See Arrouays et al. (2018) and ICOS protocol (Loustau et al. 2017) for more information. In both campaigns, the FE

225

230

fraction was then split into three subsamples to measure the C content (air-dried sample), residual water (after drying at 105°C) and soil bulk density (BD). Soil organic carbon (SOC) content ($C, \text{g kg}^{-1}$) was determined in the air-dried FE fraction by dry combustion (ISO 10694), which measures the total carbon content in the soil. Overall, in 2005 and 2019, the soil preparation and analysis were very similar. Carbonate ($\text{CaCO}_3, \text{g kg}^{-1}$) was measured by determining the loss of carbon dioxide (CO_2) after acidification with hydrochloric acid in 2019. The inorganic carbon content was also determined in 2019: when CaCO_3 content was lower than 700 g kg^{-1} , the soil inorganic carbon (SIC) content was calculated as $C = 0.12 \times \text{CaCO}_3$. When CaCO_3 content exceeded 700 g kg^{-1} , to avoid a deterioration in the accuracy of organic carbon deduced from total carbon, samples were first treated with HCl to eliminate carbonates, and then total carbon was determined as explained previously. The SOC content was then computed as the total carbon content minus the inorganic carbon content.

235

240 2.4 Soil data pre-processing

Prior to statistical analysis, missing values in the 2005 dataset were imputed using Ordinary Kriging interpolation (Goovaerts, 1997), which leverages spatial autocorrelation to provide unbiased and minimum variance estimates of missing data points. Using spatial coordinates, the target variables were estimated based on interpolated values derived from a fitted variogram model (Nugget + Spherical) and up to 35 neighbouring data points within a 100-unit radius. For the 2019 dataset, which had only a single missing value, we used the average value of the corresponding soil layer.

2.5 Soil carbon stocks calculation using the fixed-depth (FD) approach

The soil carbon stock SOC_{stock} (kg C m⁻²) across the soil layers was calculated following Poeplau et al. (2017):

$$250 \quad SOC_{stock} = \sum_{i=1}^n \frac{m_{FE_i}}{m_{soil_i}} \times BD_i \times \Delta z_i \times SOC_i \times \frac{1}{1000} \times 10000 \quad (1)$$

Where n is the number of layers in which the soil core was divided down to 60 cm, i is the layer index, m_{FE_i} (g) is the mass of fine earth in the layer, and m_{soil_i} (g) is the total soil mass of the layer (including rocks and roots), BD_i (g cm⁻³) is the bulk density of the layer, Δz_i is the layer thickness (cm), and SOC_i (g C kg⁻¹) is the SOC content in the FE fraction in the layer. The factor $\frac{1}{1000}$ converts SOC content from g kg⁻¹ to kg kg⁻¹, and the factor 10000 converts cm² to m². The bulk density in each soil layer is defined as the ratio of m_{soil_i} to the soil core volume V_{sample_i} :

$$260 \quad BD_i = \frac{m_{soil_i}}{V_{sample_i}} = \frac{m_{soil_i}}{S_i \times \Delta z_i} \quad (2)$$

where S_i is the sampled surface. Equations (1) and (2) correspond to equations (1) and (2) in Schrumpf et al. (2011) and were used to compute the stocks for the 2005 samples. We note that when combining equations (1) and (2), the mass of soil m_{soil_i} and the layer thickness Δz_i disappear. In the ICOS stock calculation protocol, the bulk density is therefore not used anymore. The SOC stocks are computed based on the surface sampled S_i and the mass of fine earth m_{FE_i} only. By further simplifying the converting factors, one gets:

$$SOC_{stock} = \sum_{i=1}^n \frac{m_{FE_i}}{S_i} \times SOC_i \times 10 \quad (3)$$

In equation (3), a term can be identified as the fine earth in each layer, $FE_i = m_{FE_i}/S_i \times 10$ (kg m⁻²), which gives the fine earth over the 0-60 cm profile:

$$275 \quad FE_{60cm} = \sum_{i=1}^n \frac{m_{FE_i}}{S_i} \times 10 = \sum_{i=1}^n FE_i \quad (4)$$

We note here that these equations are adapted for core sampling. When sampling soils with pits, some corrections need to be introduced in equations (1-3) to account for large stones and large roots in the pit. The inorganic carbon

stock SIC_{stock} is computed in a similar way as the SOC_{stock} but replacing the OC content in the FE fraction SOC_i by the inorganic carbon content SIC_i . Finally, the cumulative $SOC_{stock}^{0-60\text{ cm}}$ was computed after summing the stocks per layer.

2.6 Harmonisation of soil layers in both sampling campaigns

280 To ensure comparability between campaigns, the soil sampling depth (**Figure 2**) of each campaign was harmonised into three coarser layers: 0–5 cm, 5–30 cm, and 30–60 cm. Bulk density, rock fragments, and carbon content were aggregated using a thickness-weighted mean to account for variable layer depths, while SOC stocks and fine earth mass were calculated as cumulative sums across the respective layers.

2.7 Soil carbon stocks calculation using the equivalent soil mass (ESM) and SOC stocks changes

285 To properly estimate SOC stocks evolution, one needs to consider changes in SOC content of the soil (SOC) but also the potential changes in BD_i due to compaction or decompaction, which may change the fine earth mass FE_i in each sampling depth (Lipiec and Hatano, 2003). Additionally, soil erosion driven by rainfall or wind can export soil particles – mainly silt and clay - out of the field. Erosion is thought to be negligible at the FR-Gri site due to a slight slope and systematic winter inter-cropping. Decompaction may have happened since the site was converted
 290 to reduced tillage from 2000 onwards (Loubet et al., 2011), but compaction in subsoil may also occur due to repeated surface traffic by heavy machinery (Liebhard et al., 2025; Lu et al., 2021). To consider possible changes in BD_i , the SOC stock evolution was estimated using the equivalent soil mass method (ESM), where the SOC stock is integrated down to a varying depth corresponding to a reference soil mass that is set equal for each campaign (Ellert and Bettany, 1995; von Haden et al., 2020; Lee et al., 2009; Wendt and Hauser, 2013). This approach
 295 has the advantage of accounting for a common sampling bias with the hydraulic corer, which is soil compaction. The ESM-based SOC stock was computed using the R function “*SimpleESM*” (Ferchaud et al., 2023), which implements the classical ESM method (Ellert and Bettany, 1995) and ESM2, a model-based approach incorporating cubic splines (Wendt and Hauser, 2013). The reference fine earth mass (FE_{ref}) was derived from the median values in the 2005 dataset for the aggregated soil layers: 0–5 cm, 5–30 cm, and 30–60 cm (**Table 2**). The total FE
 300 in the 0–60 cm layer ranged from 852 to 967 kg m⁻² in 2005, and from 831 to 953 kg m⁻² in 2019 (**Table S4**).

Table 2. Reference fine earth mass (FE_{ref}) per layer used in the equivalent soil mass approach (ESM).

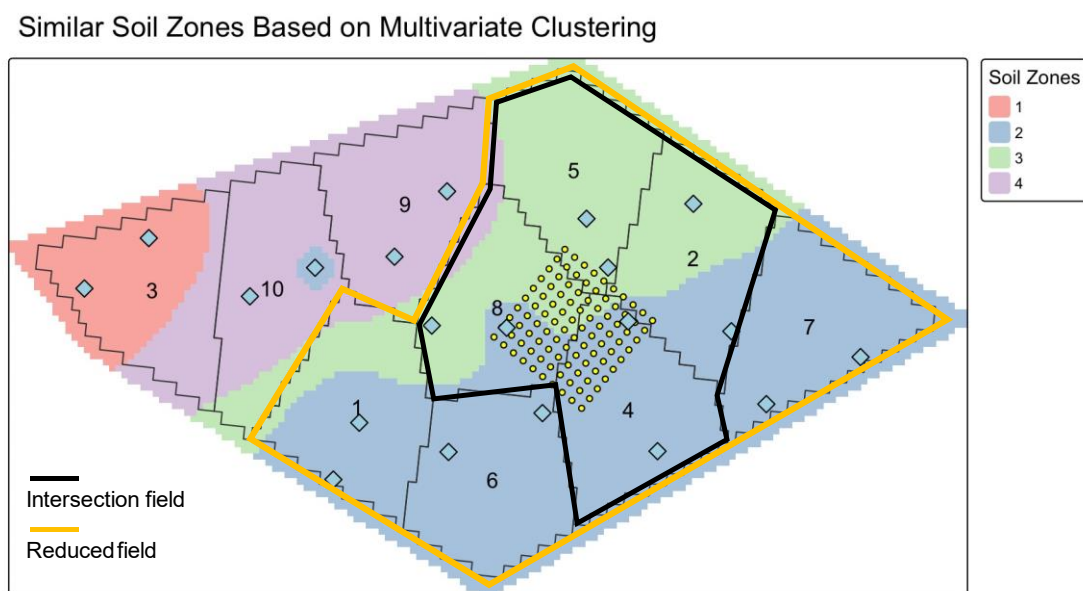
Layer	Upper depth	Lower depth	FE_{ref} kg m ⁻²
	cm		
L1	0	5	63.2
L2	5	30	372.6
L3	30	60	453.1

In the “classical” ESM approach (Ellert and Bettany, 1995), SOC stock is calculated by 1 mm increments (Autret
 305 et al., 2016; Mary et al., 2020). In brief, soil depth is discretised into elementary layers of 1 mm thickness, with FE density (g cm⁻³) and carbon content (g kg⁻¹) assigned to each 1 mm layer. Since both FE density and the SOC content are typically reported as average values over macro-layers (e.g., 0–5 cm), these values are assumed to be constant within each 1 mm sublayer. Subsequently, FE_i and SOC_{stock_i} are then computed cumulatively until the FE_{ref} is reached. This approach is referred to as “*ESM non model*” by (Peng et al., 2024). The ESM2 approach is

310 based on the "material coordinate system" (Lee et al., 2009; McBratney and Minasny, 2010) or the "cumulative
coordinates approach" (Rovira et al., 2015). This method uses a *post-hoc* model - a cubic spline interpolation - to
mathematically adjust SOC measurements to a common fine earth mass (von Haden et al., 2020; Wendt and
Hauser, 2013). As both methods yielded similar results (**Figure S7**), only ESM outcomes are reported in the fol-
lowing.

315 2.8 Spatial comparison between 2005 and 2019

To enable a reliable comparison between the 2005 and 2019 data and infer changes in SOC stocks, we minimised
the effect of spatial heterogeneity in the 2019 sampling by subsetting the strata. To address this, we first employed
a K-means-based clustering algorithm (MacQueen, 1967) to identify pedologically homogeneous zones. We used
the 2019 dataset, which offered well-distributed coverage across the study area, with each sampling point charac-
320 terised by its physical (clay and rock fragment contents, fine earth mass) and chemical properties (carbonates and
SOC content). In addition, we extracted information from the soil descriptions of each 2019 SP-I (**Table S2**),
including effective soil depth (parent material layer not included) and clay content (%). These variables were
aggregated to a depth of 60 cm using weighted mean (e.g., for carbonates) or summation (e.g., for soil mass) and
then interpolated using Inverse Distance Weighting (IDW) of power 2 (Shepard, 1968), selected as the most suit-
325 able method for interpolation given the limited number of samples ($n < 30$). The resulting raster maps were stacked
in a single raster and resampled to a common resolution. Subsequently, K-means-based clustering algorithms were
applied (with $K = 4$) using the *stats::kmeans* (R core team, 2005) to delineate zones with comparable pedological
characteristics. The number of clusters (K) was defined using the elbow within-cluster sum of squares (Thorndike,
1953). This analysis resulted in the identification of four distinct clusters, hereafter, soil zones (**Figure 3**).



330 **Figure 3.** Map showing similar soil zones derived from multivariate clustering analysis. The study area is classified into
four distinct soil zones (labelled 1–4), each representing regions with homogeneous soil properties based on statistical
clustering of multiple variables (clay content, rock fragments, carbonates, organic carbon, fine earth mass, effective soil
depth). The 2005 (yellow circles) and 2019 (blue diamonds) sampling points are superimposed together with the strata
335 (numbered polygons) defined in the 2019 sampling. Yellow polygon represents the “*Reduced field*” and black polygon
the “*Intersection field*”.

Zone 2 is characterised by deep soils (> 100 cm) with low contents of rock fragments and inorganic carbon. Zones 1 and 4 are composed of shallow soils (20–50 cm) with high concentrations of rock fragments and carbonates, and with less than 20% clay content. Zone 3 presents intermediate soil properties: soils are moderately shallow (40–60 cm) with medium levels of rock fragments and carbonates. The 2005 sampling points are located within Zones 2 and 3. Based on the soil property map, the 2019 data was subset in three different ways: (1) *Complete field* = Including all the strata and corresponding SP-I plots. (2) *Intersection field* = Including the four strata of the 2019 campaign (Strata 8, 4, 2, and 5) that intersected the 2005 sampling area. (3) *Reduced field* = Including the strata within the same soil zones within the 2005 sampling area, that is, the strata 1, 2, 4, 5, 6, 7, and 8. The *Intersection* and *Reduced* fields were chosen to ensure similar pedological properties in both campaigns. The SP-I_19 plot intersected Zone 2, while SP-20 did not fall within any of the target zones. Since both samples are part of Stratum 10, they were excluded from the analysis. All these analyses were performed using a set of R packages. For vector and raster manipulation, we used *sf* (Pebesma, 2018; Pebesma and Bivand, 2023), *raster* (Hijmans, 2010), and *stars* (Pebesma and Bivand, 2023). For inverse distance weighting (IDW) interpolation, we used *gstat* (Gräler et al., 2016; Pebesma, 2004). Plotting was carried out using *tmap* (Tennekes, 2018), and multivariate clustering was performed using *stats* (R Core Team, 2025). Effect-size analysis comparing soil variables in 2019 across the original sampling layers revealed no significant differences between the *Intersection field* and *Reduced field*, as indicated by Hedges' *g* values close to zero and confidence intervals spanning zero (**Figure S1**). In contrast, the *Complete field* and *Reduced field* exhibited significant differences in several soil variables, such as SOC and SIC content, SOC and SIC stocks, rock fraction percentage, total nitrogen content and stocks, and fine earth mass, with different differences pronounced up to 30 cm. Notably, SIC content and stocks differ consistently across all layers. Given these discrepancies in soil properties, the following sections focus on comparisons between the 2005 and 2019 campaigns within the *Reduced field* to explore the SOC changes due to its consistent soil properties.

2.9 Statistical inference for assessment of the carbon stock change

Unequal variance t-tests (Welch's t-test) were applied to assess significant differences between the two campaigns' means of SOC stocks estimated by FD and ESM approaches and other soil variables. The Welch's t-test value was calculated as:

$$t = \frac{(\widehat{X}_{2005} - \widehat{X}_{2019})}{\sqrt{\widehat{V}(\widehat{X}_{2005}) + \widehat{V}(\widehat{X}_{2019})}} \quad (5)$$

Where \widehat{X} is the estimated mean of the soil property X , $\widehat{V}(\widehat{X})$ is the estimated sampling variance of the estimated mean, and indexes stand for the campaign years. A design-based approach was used to estimate the means and sampling variances (de Gruijter et al., 2006). The sampling variances of the two campaigns were estimated separately and considered unequal. For the 2019 campaign, a stratified random sampling with equal area strata was used. With the same number of sites per stratum, the mean and the sampling variance are estimated as:

$$\widehat{X} = \frac{1}{N} \sum_{i=1}^N X_i \quad (6)$$

$$\widehat{V}(\widehat{X}) = \sum_{h=1}^H w_h^2 \widehat{V}(\widehat{X}_h) = \frac{1}{4} \sum_{h=1}^H \widehat{V}(\widehat{X}_h) \quad (7)$$

Where X_i is the measured soil property at location i , N is the total number of samples over all strata, $\widehat{V}(\widehat{X}_h)$ is the sampling variance of stratum h , $w_h^2 = \frac{1}{4}$ is the weight of stratum h , and H is the number of strata.

For systematic random sampling (2005 campaign), the mean estimate is simple (Eq. 6), but there is no unbiased estimate of the sampling variance. We implemented the approximation suggested by Brus and Saby (2016), where the systematic random sample is treated as a stratified simple random sample. The sampling units were thus clustered by 2 based on their spatial coordinates into $H = n/2$ clusters ($n = 100$) using a k -means algorithm. The 2 sampling units of a cluster were treated as a simple random sample from a stratum, and the variance was estimated with eq. (7) with $H = 50$. The weights were computed by $w_h^2 = n_h/n$, where $n_h = 2$ is the number of units per cluster. The 95% confidence interval is given by:

$$\widehat{X} \pm t_{2.5}^{N-H} \sqrt{\widehat{V}(\widehat{X}_h)} \quad (8)$$

Where $t_{2.5}^{N-H}$ is the 2.5 quantile of a t distribution where $(N - H)$ approximates the degrees of freedom. For the 2005 campaign, degree of freedom $N - H = 100 - 50 = 50$. In 2019, when the *Complete field* was considered, there were $H = 10$ strata of 2 units each, leading to a total number of sampling points $N = 20$ (called SP-I in ICOS), leading to $N - H = 10$. When part of the field was considered, both the number of samples and H diminished leading to $N - H < 10$. In 2005 and 2019, equations (7-9) were used to compute the carbon stock statistics for each sampling depth available and over aggregated layers 0-15 cm, 15-30 cm and 30-60 cm. We also computed the minimum detectable difference (MDD) based on a t-test with 95% confidence and 90% power ($\alpha = 0.05$, $\beta = 0.10$).

Finally, we performed an additional statistical analysis to quantify the magnitude of SOC stock changes between 2005 and 2019 by calculating effect sizes using Hedges' g . This metric is a standardised mean difference method that includes a correction for small sample sizes (Hedges, 1981), which was especially the case when using the Reduced and Intersection fields, leading to 14 and 8 samples, respectively. Confidence intervals for effect-size estimates were computed using 20000 nonparametric bootstraps with resampling and the bias-corrected and accelerated (BCa) method (Canty et al., 2024; Efron, 1987; Kirby and Gerlanc, 2013). Negative values of Hedges' g indicate a reduction in SOC stocks from 2005 to 2019, while positive values indicate an increase. If the confidence intervals (CIs) include zero, it suggests that there is no significant difference in SOC stocks between the two sampling years. These analyses were performed using the R package "*bootES*" (Kirby and Gerlanc, 2013).

See the equations (s1-s5) in the supplementary material.

2.10 Simulation of carbon stock evolution with the AMG model

We computed the SOC stock changes using the agricultural soil carbon model AMG (Clivot et al., 2019) to compare with measured changes in SOC stock in the surface soil layer (0-30 cm). AMG is a relatively simple soil carbon model that simulates SOC stocks by partitioning the soil carbon into three pools: (1) a pool receiving organic C inputs from crop residues, roots, and exogenous organic matter (EOM), (2) an active organic C pool subject to decomposition, and (3) a stable organic C pool. As stable C presents slow turnover, this pool is considered inert in the model, considering the timescale of the simulation – it does not decompose nor receive new C inputs.

A proportion (h_a) of C input is allocated to the active C pool, while the remaining proportion ($1 - h_a$) is mineralised. The active C pool decomposes following first-order kinetics, with a rate constant k that depends on climate variables (annual temperature, precipitation, potential evapotranspiration) and soil properties (clay content, carbonate content, pH, and C:N ratio). The C inputs to the soil include aboveground crop residues and organic amendments

from manure and slurry as listed in **Table 1**, plus the belowground crop residues estimated from allometric equations (Eq. 16) based on the aboveground biomass (Clivot et al., 2019, 2023). Roots and rhizodeposition C inputs down to a considered depth i are computed as:

$$415 \quad C_{BG(i)} = \frac{DM_{AG}}{SRR} * 0.4 * 1.65 * (1 - \beta^i) \quad (9)$$

Where DM_{AG} is the above-ground biomass, SRR is the shoot-to-root-ratio, 0.4 is the carbon content of the roots (40%), 1.65 is a factor accounting for the dead roots and rhizodeposition, assumed to be 65% of the living roots C, and $(1 - \beta^i)$ accounts for the roots' distribution in the soil, where β is a crop-dependent parameter.

420 The SOC stock changes were simulated on an annual timestep over the period 2005–2040, considering the 0-30 cm depth layer, which generally corresponds to the managed soil layer in cropland systems, where most crop roots and residue inputs occur. The baseline SOC stock was set to 8.25 kg C m⁻², based on measurements from 2005. The proportion of active C was set to 65%, as Clivot et al. (2019) proposed for agricultural fields with a long-term history of cultivation. To assess model sensitivity, we performed additional simulations varying key management and environmental factors: (1) residue returns to the soil were increased to 100%, (2) organic amendments were 425 either eliminated (set to zero) or doubled (multiplied by two), (3) meteorological conditions were held constant by repeating the 1987–2004 weather data for the 2005–2040 period, and (4) the ratio of active to stable carbon pools ($C_s = 0.65$) was varied using values of 0.63 and 0.75 taken from independent estimates on a nearby soil reported by Kanari et al (2022) to illustrate the model's response to this critical parameter.

2.11 Carbon flux balance estimations using the ICOS approach between 2006 and 2010

430 The carbon flux balance was estimated from 2006 to 2010 in Loubet et al. (2011), based on the Eddy Covariance (EC) micrometeorological method. The net biome productivity (NBP), representing the carbon balance of the field, was computed as:

$$NBP = NEE + F_{orga.fert} + F_{seeds} - F_{leach} - F_{harvest} \quad (10)$$

435 where NEE is the net ecosystem exchange of CO₂ flux over time, $F_{orga.fert}$ is the carbon input through organic fertilisation, F_{seeds} is the carbon input through seedling, F_{leach} is the organic and inorganic carbon losses by lixiviation, and $F_{harvest}$ is the carbon export through harvest. See Loubet et al. (2011) for details. We limited the carbon balance study to the 2006–2010 period published in Loubet et al. (2011). Indeed, computing the full period 2005–2019 carbon balance requires filling a year gap in 2018 and processing the leaching flux, which implies crop and leaching modelling, as well as an uncertainty analysis that goes beyond the scope of this manuscript.

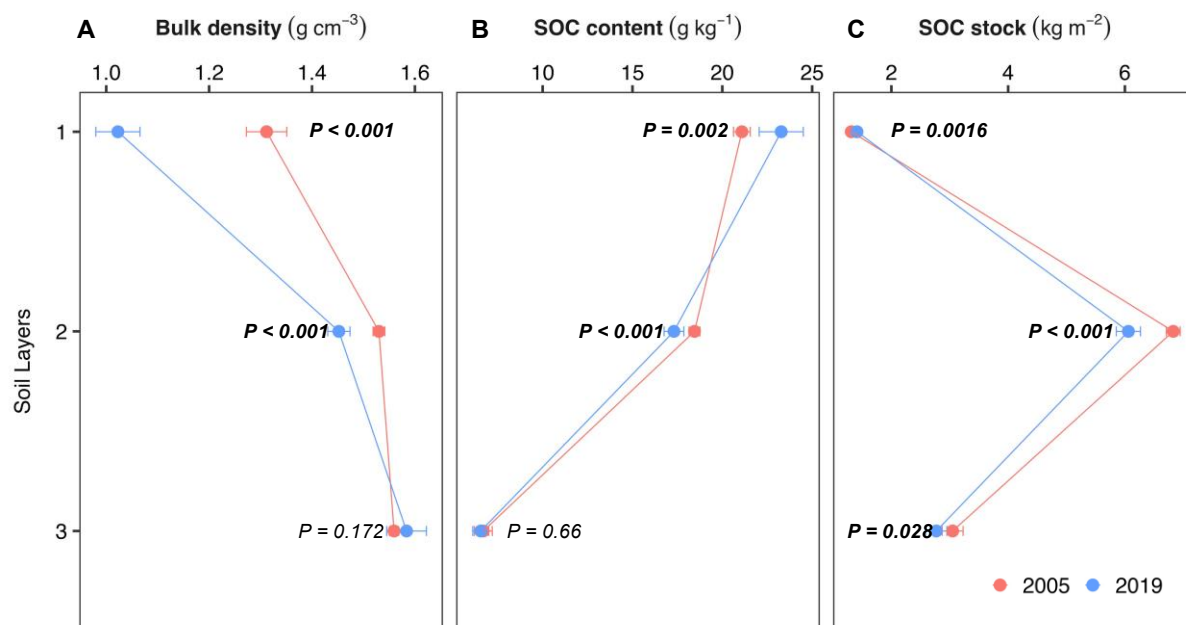
440 3 Results

3.1 Summary statistics of soil properties

The 2005 campaign was already published by Schrupf et al. (2011), but the 2019 campaign has yet to be published. The 2019 campaign covered a much larger area than the 2005 campaign, which included a small section on the northeast side of the field with shallow (~40 cm depth) and calcareous soils, as pointed out by Loubet et al.

445 (2011) and as visible in **Figure S2-S3**. The shallow soil zone (e.g., strata 3, 9, and 10) shows high rock fractions (RF), ranging between 10% and 15%. In contrast, the deep soil zones (e.g., strata 1, 4, 6, 7) have much lower RF, ranging from 0.6% to 2%. The distribution of RF and inorganic C per layer across the 2019 area can be found in **Figure S4**. The area sampled in 2005 (**Figure S5**) showed a rock fraction smaller than a few per cent, as also reported by Schrumpf et al. (2011). The proportion of the fine earth (FE_{prop}) in the soil ranged from 0.92 to 0.99
 450 after harmonising the data into three common depth intervals (**Table S4, Figure S4**). In the *Reduced field*, changes in the proportion of the fine earth between 2005 and 2019 were small and statistically non-significant (differences < 1%), which was not the case in the *Complete field*, which showed a significant difference of around 3% (**Table S5**).

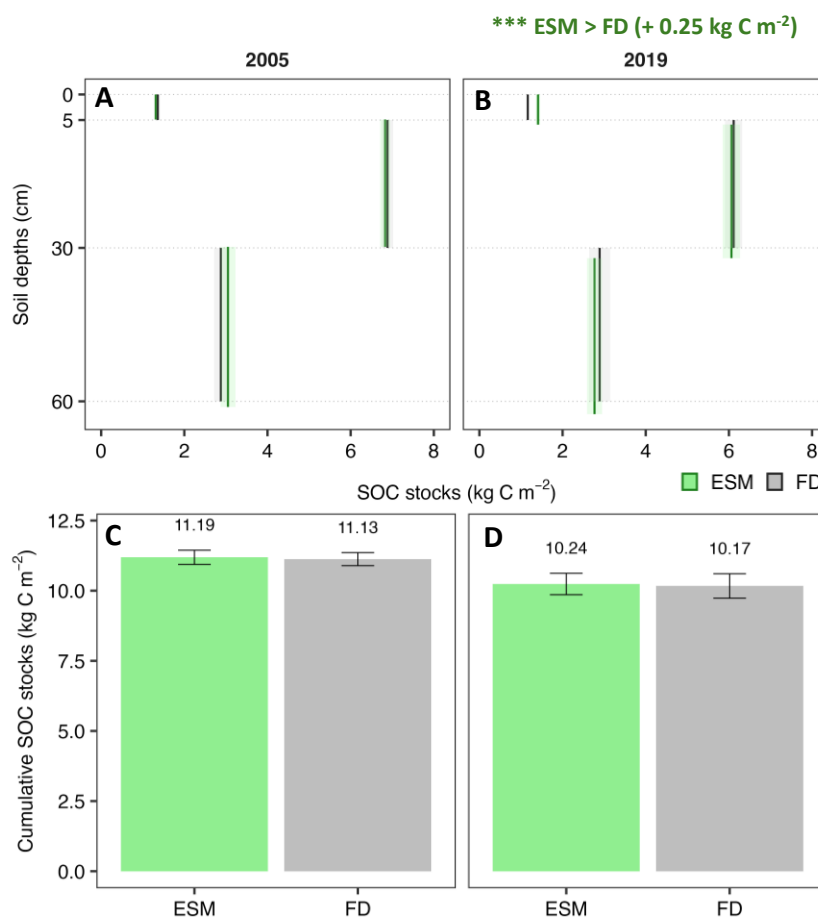
Statistical analysis confirmed a significant decompaction from 2005 to 2019, evidenced by a reduction in bulk density within the *Reduced field*, particularly in the 0-5 cm ($p < 0.001$) and 5-30 cm ($p < 0.001$) layers (**Figure 4, Table S5**). BD decreased by ~25% in the 0-5 cm layer and by ~5% in the 5-30 cm layer, while the 30–60 cm layer presented a slight but non-significant increase. Similar results were observed for the fine earth density (Table S4). For the entire 0-60 cm profile, the average soil stock (FE_{0-60cm}) in 2005 was 882.5 kg m^{-2} , which was about 5% greater than in 2019 (840.1 kg m^{-2}), while the soil mass in the 0-5 layer decreased by approximately 25%. The
 460 SOC contents varied from 2005 to 2019 (**Figure 4, Table S5**). In the 0–5 cm layer, SOC contents were significantly higher in 2019 than in 2005 by around $2.2 \pm 0.57 \text{ g C kg}^{-1}$ ($p = 0.002$). In contrast, SOC content in the 5-30 cm layer was significantly lower by 6.2% in 2019 compared to 2005, with a mean difference of $-1.14 \pm 0.28 \text{ g C kg}^{-1}$ ($p < 0.001$). In the 30–60 cm layer, SOC contents remained statistically unchanged $-0.14 \pm 0.31 \text{ g C kg}^{-1}$, $p = 0.66$).



465 **Figure 4.** Mean of bulk density and soil organic carbon (SOC) contents and stocks with their corresponding confidence intervals (CIs) in the 2005 and 2019 campaigns across three soil layers (0-5, 5-30, 30-60 cm). Only the “*Reduced Field*” is presented.

470 **3.2 Differences between FD and ESM-based SOC stocks**

As no differences were detected between the ESM (non-model) and ESM2 (cubic spline) approaches (**Figure S6**), only ESM-based results are presented hereafter. FD and ESM approaches were statistically similar in 2005 across the three soil layers (**Figure 5A**), but we found significant differences in the first soil layer ($p < 0.001$) in 2019 (**Figure 5B**). However, both approaches did not differ when comparing the cumulative SOC stocks up to ~60 cm (all $p > 0.5$, **Figure 5C-D**).



480 **Figure 5. Soil Organic Carbon (SOC, kg C m⁻²) stocks and corresponding confidence intervals (error bars) in Fixed**
Depth (FD) and Equivalent Soil Mass (ESM) approaches. Panel A) Solid lines (vertical) represent the mean SOC stocks
across the entire depth range, while shaded ribbons indicate the upper and lower CIs. The dashed grey (horizontal) line
represents the fixed soil depth aggregated into 0-5, 5-30, and 30-60 cm. If the thickness of the ESM-adjusted depth falls
outside the upper or lower bounds of the fixed soil depth, it indicates that a depth adjustment was made during the
ESM computation. Panel B) Cumulative SOC (kg C m⁻²) along with their corresponding confidence intervals (error
bars). Asterisks denote significant differences between both campaigns: $P < 0.0001$ (*), $P < 0.001$ (**), $P < 0.05$**
(*).

485 **3.3 Soil carbon stock changes over time**

The mass-equivalent depth (**Figure 6A**) varied across all layers according to the reference soil mass shown in **Table 1**. On average, the mass-equivalent depths in 2019 were 0–6 cm, 6–33 cm, and 33–65 cm. In 2005, the soil depth adjustment was minimal compared to the sampling depth, with an increase of 2 ± 0.7 cm in the third layer (30-62 cm). The ESM estimates indicated a higher SOC stock 2019 than in 2005 ($\Delta\text{SOC} = 0.1 \pm 0.02$ kg C m⁻²) in

the sampling depth of 0–5 cm (**Figure 6B**). The second layer (sampling depth of 5–30 cm) showed a lower SOC stock in 2019, with a Δ SOC of about $0.8 \pm 0.10 \text{ kg m}^{-2}$. In the deeper layer (sampling depth of 30–60 cm), ESM-based SOC stock changes showed a pronounced reduction of about $0.28 \pm 0.11 \text{ kg m}^{-2}$. Effect-size comparisons between the two campaigns across the three layers are shown in **Figure S7**. In addition, ESM-based SOC stock changes were computed across the seven-reference soil mass corresponding to the seven layers sampled in 2005 campaign (**Figure S8**). The results show that SOC stocks in 2019 were higher in the layer L1 (~0-5 cm), then decreased between layer L3 and L5 (~20 and ~40 cm), before increasing again in layers L6 and L7 (~ 40 - 60 cm).

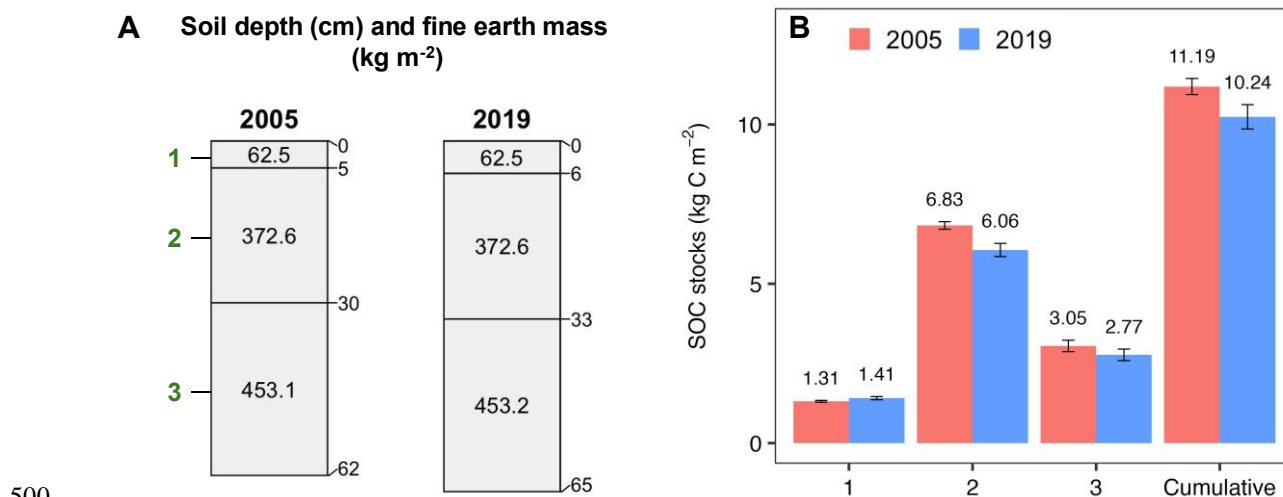


Figure 6. Mean soil organic carbon (SOC) stocks (kg C m^{-2}) estimated using the Equivalent Soil Mass (ESM), along with their corresponding confidence intervals (error bars), for the 2005 and 2019 campaigns. Adjusted soil depth (cm) and fine earth mass (kg m^{-2}) are also shown in Panel A. Commutation made for the “*Reduced Field*” where only seven strata from the 2019 dataset with pedological characteristics similar to the 2005 area were selected. Asterisks denote significant differences between both campaigns: $P < 0.0001$ (***), $P < 0.001$ (**), $P < 0.05$ (*).

3.4 Cumulative SOC stocks

Across the 13.25-year monitoring period, the cumulative SOC stocks up to the sampling fixed-depth 0-60 cm exhibited a statistically significant decline ($p < 0.05$) of around $0.95 \pm 0.22 \text{ kg C m}^{-2}$ ($p < 0.001$; MDD < observed differences, **Table 3**). A similar decline was found using the ESM and the FD. Overall, both SOC estimation approaches indicate an average SOC loss of approximately $72 \pm 16 \text{ g C m}^{-2} \text{ yr}^{-1}$ over the 13.25-year period. In the *Complete field*, the ESM-based SOC stock difference MDD exceeded the observed difference, indicating a potential for a Type II error (failing to detect a real effect). In terms of proportional reduction relative to the 2005 baseline, ESM-based SOC stocks decreased by -8.2% in the $\sim 0\text{--}30 \text{ cm}$ layer and -8.5% in the $\sim 0\text{--}60 \text{ cm}$ layer. These losses translate to annualised losses of approximately -0.62% to $-0.89\% \text{ yr}^{-1}$, when referenced to the 2005 SOC stocks baseline.

Table 3. Summary of soil organic carbon (SOC) stock changes between 2005 and 2019 in the “Reduced field” at the FR-Gri site, assessed for the 0–30 cm and 0–60 cm soil layers using both the Equivalent Soil Mass (ESM) and Fixed-Depth (FD) approaches. SOC changes are reported in absolute terms (kg C m⁻²) following by their standard error, relative change (% of initial stock), and as annualised rates. The Minimum Detectable Difference (MDD) represents the smallest true difference that can be statistically detected given the observed variability and sample size. If the observed ΔSOC exceeds the MDD and $p < 0.05$, the change is considered detectable. If ΔSOC is less than the MDD, the change is not statistically distinguishable. A large MDD reflects high variability or limited sensitivity, whereas a small MDD indicates high precision in detecting SOC changes. These estimates were also used as input parameters for the AMG model simulations.

Metric	Equivalent Soil Mass		Fixed depth	
	~ 0-30 cm * 435.1 kg m ⁻²	~ 0-60 cm 887.6 kg m ⁻²	0-30 cm *	0-60 cm
2005 SOC stocks (kg C m ⁻²)	8.14 ± 0.06	11.19 ± 0.13	8.25 ± 0.08	11.12 ± 0.12
2019 SOC stocks (kg C m ⁻²)	7.47 ± 0.09	10.24 ± 0.16	7.28 ± 0.09	10.17 ± 0.18
ΔSOC (kg C m ⁻²)	-0.67	-0.95	-0.97	-0.96
Standard Error difference (kg C m ⁻²)	0.11	0.04	0.12	0.04
Lower CI difference (kg C m ⁻²)	-0.90	-1.37	-1.22	-1.40
Upper CI difference (kg C m ⁻²)	-0.44	-0.53	-0.72	-0.51
<i>P values</i> (two-sided)	< 0.001	< 0.001	< 0.001	< 0.001
Minimum Detectable Difference (kg C m ⁻²)	0.38	0.71	0.41	0.76
SOC stock change (% of initial Stock)	-8.2%	-8.5%	-11.8%	-8.6%
SOC stock change (% initial Stock yr ⁻¹)	-0.62% yr ⁻¹	-0.65% yr ⁻¹	-0.89% yr ⁻¹	-0.64% yr ⁻¹
SOC stock change (per mil initial Stock yr ⁻¹)	-6.2‰ yr ⁻¹	-6.5‰ yr ⁻¹	-8.9‰ yr ⁻¹	-6.4‰ yr ⁻¹

* SOC stocks from 2005 at 0-30 and 0-60 cm were inserted as input variables in the AMG model.

3.5 Comparison of measured SOC stock changes with estimations obtained with the AMG model

The AMG model was used to simulate the soil organic carbon stock evolution from 2005 to 2040 in the 0-30 cm layer, based on the cropping system, imports and exports, computing the plant residues return based on allometric relationships. Under current cropland management practices, the model evidenced a declining trend of SOC stocks (Figure 7), which aligns with the decrease observed with the ESM approach in the 0-30 cm layer. Under current management, AMG models that SOC decreased from 8.24 kg C m⁻² in 2005 to 7.25 kg C m⁻² by 2019, reflecting a cumulative loss of approximately 0.99 kg C m⁻² (-12%) over 13.25 years. SOC stocks appear to approach a quasi-steady-state from 2027 onwards, with fluctuations of ±0.02 to ±0.04 kg C m⁻² yr⁻². By 2040, SOC stocks are projected to decrease to 6.94 kg C m⁻², representing an approximate 15% reduction from the 2005 baseline. Both the AMG model and measured SOC stocks were consistent with the flux balance approach reported by Loubet et al. (2011), during the early period from 2006 to 2010. The overall loss over a 22-year period (2005-2027) would then be of around 1.3 kg C m⁻², or 13 Mg C ha⁻¹, which amounts to 0.059 Mg ha⁻¹ yr⁻¹. Overall, the sensitivity analysis across five scenarios shows the same declining patterns in SOC, with cumulative losses ranging from 5 to 18% by 2019, and from 6 to 23% by 2040. Increasing the residue return leads to a stabilisation of the SOC stock near 7.15 instead of 6.95 kg C m⁻², while doubling the organic carbon amendment would lead to an equilibrium of 7.48 kg C m⁻². On the contrary, suppressing the organic carbon amendment would lead to a stabilisation of 6.34 kg C m⁻².

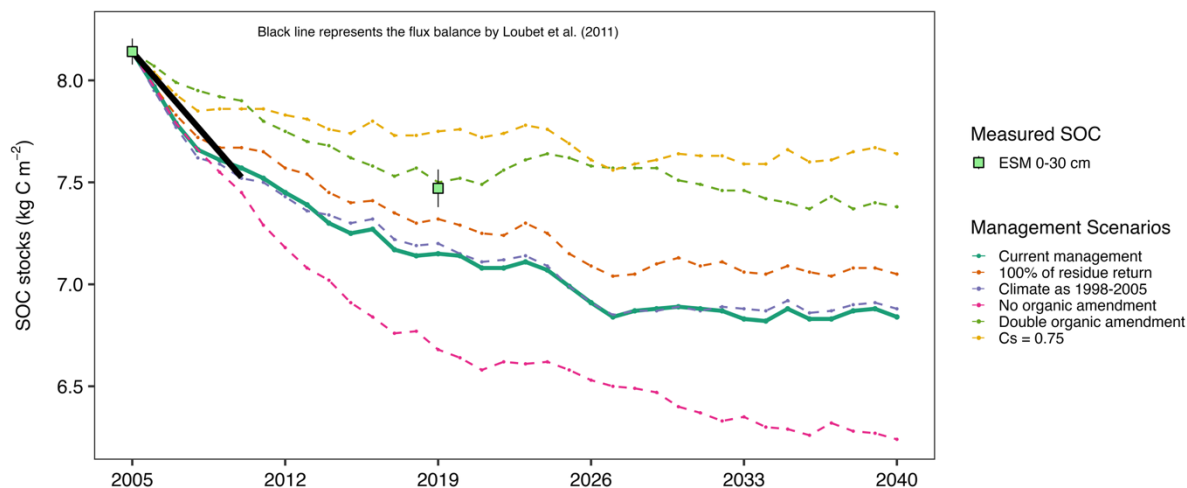


Figure 7. Soil organic carbon (SOC) stock in the 0-30 cm depth as simulated by the AMG model (plot lines), measured by soil sampling in 2005 and 2019 and computed using the equivalent soil mass (ESM; light-green square). The error bars show the sampling standard error. The 2019 SOC stock is given for the “Reduced field” only. Flux balance over the 2006-2010 period (black line) as published in Loubet et al. (2011), scaled to start at the measure SOC stock in 0-30 cm.

4 Discussion

4.1 Effects of sampling depth and computation methods on organic carbon stock changes evaluation

Our results reveal that cumulative SOC stock changes between 2005 and 2019 under reduced tillage management were similar when using either the FD or ESM approach, differing by only 3% in the 0–60 cm sampling layer ($p > 0.80$). Previous studies have documented misleading interpretations of SOC stock increases with reduced or no-tillage when using the FD approach at shallow depths (≤ 30 cm) (Du et al., 2017; Xiao et al., 2020). Our results support this in the 0-5 cm layer, where FD indicates SOC stock losses while ESM shows gain (**Table S5, Figure S7**). Indeed, FD approaches are prone to bias when soil bulk density or SOC content changes, irrespective of the soil management (von Haden et al., 2020). Because BD often varies with management in agricultural soils, especially at shallow depths (≤ 30 cm), multilayer sampling and equivalent soil mass approaches are essential to capture the temporal response of SOC stock in shallow layers (Wendt and Hauser, 2013; Xiao et al., 2020). At the FR-Gri site, the topsoil (0–15 cm) is frequently disturbed by shallow tillage using a stubble cultivator or clod crusher, and deep tillage operations have occasionally been applied to depths of up to 40 cm. In addition to residue return, these practices influence BD and soil mass distribution, particularly within the upper 40 cm of the profile. Additionally, the potential compaction caused by repeated machinery traffic cannot be excluded (Hamza and Anderson, 2005), since the compaction tends to accumulate over time below 40 cm due to limited tillage operations of the subsoil (Zhang et al., 2024). Roots may also alter BD, including in subsurface layers, by modifying the physical properties (e.g., aggregation, porosity) as roots efficiently explore deeper layers. In the FR-Gri site, we find a significant decrease of BD in the 0-5 cm and 5-30 cm layers and no significant change in the lower layer (30-60 cm) (**Table S4**). Likewise, roots may contribute to subsoil SOC stocks through root growth, biomass accumulation, and rhizodeposition. The rhizodeposition process may account for up to 65% of root C and ~10% of total photosynthesised C, as shown for maize (Tardieu, 1988) and wheat (Zhang et al., 2020; Zou et al., 2022), the main crops at the

575 FR-Gri site. Fan et al. (2016) reported that approximately 95% of root biomass lies above 100 cm. In our field, 20% of the SOC stock changes occurred in the 30-60 cm layer, confirming that sampling to at least 60 cm better captures root-related C inputs and reduces SOC bias estimate, as also emphasised by Baker et al. (2007) and Wendt and Hauser (2013). Furthermore, SOC stock estimates in deeper and multiple layers provide valuable insights into SOC dynamics across the profile, as mineralised carbon may percolate and accumulate in subsoil layers (Rumpel and Kögel-Knabner, 2011).
580

4.2 Possible causes of the observed SOC stock changes over 13.25 years

SOC stock losses in cropland systems under various management practices have been widely reported in European studies (De Rosa et al., 2024). A major cause of carbon losses is the imbalance between carbon imports and exports, which progressively leads to a shift in the carbon stock from one state to a new one, higher if the imbalance is an excess of imports or lower in the opposite case (Ingwersen et al., 2024; Poyda et al., 2019). Over the 13.25-year period (2005–2019), the FR-Gri site has experienced a decrease in SOC stock of 0.95 kg C m^{-2} [95% CI: 0.51-1.4]. Our study evidenced that C losses in the intermediate soil layers (5–40 cm) are not offset by gains elsewhere down to 60 cm depth (~0-5 and 40-60 cm). On average, the system implemented at FR-Gri led to a carbon stock decrease of $72 \pm 16 \text{ g C m}^{-2} \text{ yr}^{-1}$ over the 13.25 years in the ~0-60 cm soil layer, irrespective of the SOC estimation method. Our hypothesis is that SOC decline is primarily related to a long-term imbalance between carbon imports, limited by reduced crop residue return, and high biomass exports. The FR-Gri site has been under continuous cropland management for at least over 100 years, with reduced tillage and crop rotation introduced in the past two decades. In the 1980s, the field received an unquantified but large amount of organic matter inputs from wastewater treatment plants. Moreover, since 2004, increased export of wheat straw for bioenergy has reduced crop residue return, while organic amendments were limited (Table 1). This shift in management practices may have contributed to a long-term imbalance between C imports and exports, leading to SOC stock declines since, on average, the field exports were around threefold higher than imports and twice higher than the import and aerial residue return combined. The AMG simulations corroborate this hypothesis, showing a decrease mainly explained by the low residue return and limited organic C application, while the meteorology ($+0.3^\circ\text{C}$ when comparing the period of 30 years before 2005 and the period 2005-2019) does not have a significant effect on the soil C stock (Figure 7).
590
600

The initial high SOC stocks may explain the observed declining trend at our site, as sustaining such high levels is difficult even with substantial organic inputs. In terms of soil processes, SOC stock declines during that period may reflect an imbalance between SOC mineralization and immobilization rates likely triggered by high fresh plant inputs with low C:N ratio, organic amendments, and nitrogen-rich fertilisation (193 kg N ha^{-1}) in combination with climate drivers – notably elevated temperatures – that favour mineralization over immobilization (Bernard et al., 2022; Ceschia et al., 2010; Loubet et al., 2011). Mary et al. (2020) reported stable SOC stocks over 45 years in a winter wheat–maize rotation, with SOC gains in the surface layer (0–10 cm) offset by losses in deeper layers (10–30 cm), regardless of tillage intensity. However, unlike our study, their maize was not harvested for silage, which likely resulted in higher residue returns, and the initial soil C stock was also smaller. Dimassi et al. (2014) observed similar SOC stock declines (-0.018 to $-0.76 \text{ kg C m}^{-2} \text{ yr}^{-1}$) in the 0–30 cm layer under reduced residue returns and when maize was removed from the rotation. Both studies support our findings that reduced residue return and specific crop choices, such as silage maize, can significantly lower SOC stocks in cropland systems.
605
610

Keel et al. (2019) reported ESM-based SOC stock losses ranging from 0.01 to 0.135 kg C m⁻² yr⁻¹ across various crop systems in Switzerland, with an average loss of 0.034 kg C m⁻² yr⁻¹ in the topsoil (~0–20 cm). Their highest SOC stock losses were observed under a crop rotation similar to that of FR-Gri, with a comparable initial stock (~7 kg C m⁻² in the 0–20 cm layer), but implemented on an Orthic Luvisol. We notice that their C inputs from residue return and organic fertilisation (0.090–0.32 kg C m⁻² yr⁻¹) are comparable to ours (0.265 ± 0.030 kg C m⁻²), but they attributed the C losses to the recent grassland (with high SOC stock) to cropland (with low SOC stock) conversion, which may explain the doubled carbon stock change compared to this study.

The results from the AMG model application, which accounts for carbon residue return, imports and exports, reproduce the trend of observed SOC stock declines, though with a higher decline than the observed one, providing evidence that the system is not in carbon equilibrium and that this imbalance is the most plausible cause of the observed changes (**Figure 7**). Furthermore, the AMG simulation suggests that the SOC stock should diminish at the same rate until 2027 and then stabilise. A sensitivity analysis shows that increasing the residue return would lead to a stabilisation of the SOC stock to 7.2 kg C m⁻², instead of 6.95 kg C m⁻², while doubling the organic carbon amendment would lead to an equilibrium of 7.5 kg C m⁻². On the contrary, suppressing the organic carbon amendment, which may be a reality with the installation of a biogas plant on the farm, would lead to a stabilisation of 6.3 kg C m⁻². However, although not explicitly simulated in our study, digestate residues derived from biogas production could serve as an alternative organic amendment. While this residue typically contains lower content of labile organic carbon compared to fresh organic material, the remaining organic material tends to be more chemically recalcitrant and resistant to microbial decomposition. As a result, their incorporation in the soil may contribute to slight, but persistent, increases in SOC stocks over time (Keel et al., 2025; Thomsen et al., 2013).

The integrated carbon fluxes from 2006 to 2010 (Loubet et al., 2011) confirm a carbon loss from the soil similar to the AMG simulations during that period (**Figure 7**). Although the uncertainties on the integrated carbon fluxes are very large, the convergence between the two approaches corroborates a large soil carbon loss in the years 2005–2010, which is consistent with the small organic carbon fertilisations and residue return during that period (**Table 1**). We also note that the yearly carbon loss from Loubet et al. (2011) is not significantly different from the yearly carbon soil destocking found in the present study. In the north-western part of Switzerland, in a Cambisol soil, Leifeld et al. (2011) also compared the integrated carbon fluxes and soil sampling methods over 5 years on an intensive and an extensive grassland, both recently converted from intensive cropland. They concluded that the large uncertainties in both methods prevented detecting a significant change over 5 years in the intensive field. On the contrary, in the extensive field, they found a significant decrease of the SOC stock of -0.217 ± 0.143 kg C m⁻² yr⁻¹ by soil sampling, but a lower loss of -0.065 ± 0.092 g C m⁻² yr⁻¹ based on the integrated carbon fluxes method.

4.3 Uncertainties in soil carbon stock changes

We recognise the importance of distinguishing a true SOC stock change from artefacts introduced by differences in sampling designs in 2005 and 2019. To address this, the clustering of the soil based on 2019 soil properties (**Figure 3**) provides an objective way to subset the 2019 dataset to compare with the 2005 campaign over a similar soil condition. The data-driven area selection corroborates the farmer's expert knowledge of the field heterogeneity. The robustness, across both design- and model-based approaches, alongside the clustering of the soil properties

to identify distinct soil groups, increases our confidence that the observed differences reflect real changes in SOC stocks over time.

In the *Reduced field*, the observed SOC stock change between 2005 and 2019 in the 0-60 cm layer was $-0.95 \pm 0.22 \text{ kg C m}^{-2}$, exceeding the minimum detectable difference (MDD) of 0.73 kg C m^{-2} ($p < 0.01$), and this represents both significant and detectable changes given our sample size and design. In contrast, the *Complete field* did not show the same pattern, as the observed SOC changes fell below the MDD, indicating that the changes detected between 2005 and 2019 could be masked by spatial heterogeneity. Therefore, the results using the *Complete field* should be considered with caution due to the potential for Type II error (failing to detect a real effect). The larger MDD when all strata are included in our comparisons reflect increased soil heterogeneity, particularly related to the potential presence of Calcisol (shallow soil with high rock fragments and SIC content) on the north-western part of the field. These factors not only affect the soil bulk density and fine earth mass, but also the soil capacity in stabilising carbon through the positive interactions between Calcium (Ca) and soil organic matter (Kleber et al., 2021).

Additional uncertainty on the overall SOC stock change at the site may come from inorganic carbon losses. Indeed, previous measurements of carbon leaching at the FR-Gri site indicated that inorganic carbon, whose stock change could not be evaluated with the 2005 sampling data, may also contribute to significant soil carbon losses. Kindler et al. (2011) showed that, in 2010, the site was losing $28 \text{ g C m}^{-2} \text{ yr}^{-1}$ through leaching with a contribution of $21 \text{ g C m}^{-2} \text{ yr}^{-1}$ as dissolved inorganic carbon (DIC). Inorganic carbon leaching hence dominates at the site, with 75% of the leached C being inorganic, indicating a clear carbonate dissociation to DIC leaching, due to H^+ . Although not measured directly as a soil stock change, we can therefore evaluate that carbonate leaching would lead to an additional inorganic soil carbon loss of $21 \text{ g C m}^{-2} \text{ yr}^{-1}$, leading to a total of $72 + 21 = 93 \text{ g C m}^{-2} \text{ yr}^{-1}$ carbon loss. The inorganic carbon loss would therefore represent a very significant amount of 22% of the total carbon lost from the field, which could be induced by high nitrogen fertilisation (193 kg N ha^{-1} as half organic, half mineral, Table 1) and base cations exports by harvest (Raza et al., 2021; Song et al., 2022; Zamanian et al., 2021). We should however bear in mind that even if C is lost by DIC-DOC leaching from the 0-60 cm layer, it may lead to a deep C sequestration by formation of secondary CaCO_3 (An et al., 2019; Liu et al., 2022).

5 Conclusions

A significant decompaction of the 0-5 cm soil layer was observed over the 13.25 years in this crop field, with an estimated 22% decrease in bulk density in the 0-5 cm layer and a 5% decrease in the 5-30 cm layer. This decompaction is likely due to reduced deep tilling and increased intercropping since 2004. However, despite the higher SOC content in 2019, the SOC stocks only increased in the 0-5 cm layer, but decreased in the 5-30 cm layer, with no changes in the 30-60 cm layer. Consequently, cumulative SOC stocks in the 0-60 cm layer decreased by $0.95 \pm 0.22 \text{ kg C m}^{-2}$, as estimated by the equivalent soil mass approach. As we observed a similar decrease when using a fixed depth approach in the 0-60 cm layer, we conclude that sampling at a depth of 60 cm in agricultural soils is a good way to minimise biases in soil carbon stock evolution estimates.

The annual decrease of cumulative SOC stock was $72 \pm 16 \text{ g C m}^{-2} \text{ yr}^{-1}$, equivalent to a $-0.65\% \text{ yr}^{-1}$ rate of decline. This rate is consistent with earlier studies and supported by the AMG model simulation and flux balance approach over the 2005-2010 period for our site. Our study, therefore, suggests that reduced tillage, intercropping, and organic fertilisation may not be sufficient to prevent soil carbon losses when the initial SOC stock is high, as

in our site. As confirmed by other studies, the losses observed here highlight the difficulty of achieving the 4-per-mille aspirational target in cropping systems representative of the Parisian Basin, which are characterised by relatively large SOC stocks and large exports.

695 While our study detected SOC changes between 2005 and 2019, important uncertainties remain. Notably, the shift from a regular-grid design in 2005 (N = 100, nested within the 2019 footprint) to a stratified random design in 2019 (N = 20 covering the entire C-flux footprint) may introduce artefacts related to soil heterogeneity and reduced statistical power. This calls for additional campaigns in the future with the same sampling design as in 2019. According to the AMG model runs, a change of around 0.3 kg C m⁻² is expected between 2019 and 2028, which would be just above the standard error difference of 0.22 kg C m⁻² found here, indicating that a sample in 2028
700 would be meaningful.

These uncertainties call for standardised, high-quality monitoring protocols such as those developed by the ICOS research infrastructure. Consistent sampling methodologies over time are needed to reliably assess the long-term impact of crop management on SOC stocks at sites like FR-Gri, and to improve our understanding of carbon dynamics in cropland systems. Integrating SOC stock data with CO₂ flux measurements will be crucial to exploring
705 the underlying processes driving SOC changes.

Acknowledgements

We acknowledge the AgroParisTech Grignon farm and its director, Dominique Tristant, for letting us access their field and providing information on practices and yields, the direction of the infrastructure of INRAE for funding the ICOS FR-Gri site, and EU projects CarboEurope, NitroEurope and ECLAIRE for funding this work. Data
710 processing, including the sample analysis, was supported by the ICOS Ecosystem Thematic Centre. G.N. acknowledges Horizon Europe funding (Open-Earth-Monitor Cyberinfrastructure project, 101059548). D.P. thanks the support of the ITINERIS Project (IR0000032 - CUP B53C22002150006) funded under the EU - Next Generation EU Mission 4. B.W. thanks the support of the exploratory research program FairCarboN funded by the Agence Nationale de la Recherche under the France 2030 program, reference ANR-22-PEXF-0002 – projet ALAMOD.

715 We greatly acknowledge Marion Schruppf from the Max Planck Institute and her team for sharing the 2005 soil sampling data. We also thank Eric Larmanou for helping in the field during the soil sampling campaign in 2005.

Code/Data availability

The 2019 campaign report and data are accessible on the ICOS carbon portal (Buysse et al., 2025) and there
720 <https://traitementinfosol.pages.mia.inra.fr/icos/FR-GriCarbonReportv2.html>. The 2005 campaign data are accessible as an Asset. The script and all data are given as Assets.

Authors contribution

BL conceptualised, supervised, acquired the funding for the study and administered the project. BL and MG co-wrote the original draft of the manuscript with contributions from all co-authors and revised it. NS and BW provided the formal analysis, provided the statistical expertise and scripts to compute the carbon stocks in the original
725 manuscript, and co-wrote the manuscript. PB made the soil sampling and data curation for the 2019 campaign,

730 curated the crop management data and reviewed the manuscript. JPC and NS participated in the ICOS database data curation. CD managed the soils storage in 2019, contributed to data curation, and reviewed the manuscript. CJ provided expertise on the soil sampling methodology. CK made data curation on the crop management data and reviewed the manuscript. FL computed the AMG and reviewed the manuscript. BW and JLME provided expertise on the ESM methodology and reviewed the manuscript. SL participated in data curation and reviewed the manuscript. DL and DP conceptualised the data acquisition and reviewed the manuscript. GN participated in the data curation. DA initiated the project, conceptualised, developed and provided expertise on the methodology and revised the manuscript.

Competing interests

735 The authors declare that they have no conflict of interest.

References

- An, H., Wu, X., Zhang, Y., and Tang, Z.: Effects of land-use change on soil inorganic carbon: A meta-analysis, *Geoderma*, 353, 273–282, <https://doi.org/https://doi.org/10.1016/j.geoderma.2019.07.008>, 2019.
- 740 Antón, R., Arricibita, F. J., Ruiz-Sagasetta, A., Enrique, A., de Soto, I., Orcaray, L., Zaragüeta, A., and Virto, I.: Soil organic carbon monitoring to assess agricultural climate change adaptation practices in Navarre, Spain, *Reg Environ Change*, 21, <https://doi.org/10.1007/s10113-021-01788-w>, 2021.
- Arrouays, D., Saby, N. P. A., Boukir, H., Jolivet, C., and Rati: Soil sampling and preparation for monitoring soil carbon, *Int Agrophys*, 32, 633–643, <https://doi.org/10.1515/intag-2017-0047>, 2018.
- 745 Aubinet, M., Moureaux, C., Bodson, B., Dufranne, D., Heinesch, B., Suleau, M., Vancutsem, F., and Vilret, A.: Carbon sequestration by a crop over a 4-year sugar beet/winter wheat/seed potato/winter wheat rotation cycle, *Agric For Meteorol*, 149, 407–418, <https://doi.org/10.1016/j.agrformet.2008.09.003>, 2009.
- Autret, B., Mary, B., Chenu, C., Balabane, M., Girardin, C., Bertrand, M., Grandeau, G., and Beaudoin, N.: Alternative arable cropping systems: A key to increase soil organic carbon storage? Results from a 16 year field experiment, *Agric Ecosyst Environ*, 232, 150–164, <https://doi.org/10.1016/j.agee.2016.07.008>, 2016.
- 750 Baker, J. M., Ochsner, T. E., Venterea, R. T., and Griffis, T. J.: Tillage and soil carbon sequestration - What do we really know?, *Agric Ecosyst Environ*, 118, 1–5, <https://doi.org/10.1016/j.agee.2006.05.014>, 2007.
- Batjes, N. H.: Total carbon and nitrogen in the soils of the world, *Eur J Soil Sci*, 47, 151–163, <https://doi.org/DOI.10.1111/j.1365-2389.1996.tb01386.x>, 1996.
- 755 Baveye, P. C., Berthelin, J., Tessier, D., and Lemaire, G.: The “4 per 1000” initiative: A credibility issue for the soil science community?, *Geoderma*, 309, 118–123, <https://doi.org/https://doi.org/10.1016/j.geoderma.2017.05.005>, 2018.
- Beem-Miller, J. P., Kong, A. Y. Y., Ogle, S., and Wolfe, D.: Sampling for Soil Carbon Stock Assessment in Rocky Agricultural Soils, *Soil Science Society of America Journal*, 80, 1411–1423, <https://doi.org/10.2136/sssaj2015.11.0405>, 2016.
- 760 Bernard, L., Basile-Doelsch, I., Derrien, D., Fanin, N., Fontaine, S., Guenet, B., Karimi, B., Marsden, C., and Maron, P.: Advancing the mechanistic understanding of the priming effect on soil organic matter mineralisation, *Funct Ecol*, 36, 1355–1377, <https://doi.org/10.1111/1365-2435.14038>, 2022.
- Brisson, N., Mary, B., Ripoche, D., Jeuffroy, M. H., Ruget, F., Nicoullaud, B., Gate, P., Devienne-Barret, F., Antonioletti, R., Durr, C., Richard, G., Beaudoin, N., Recous, S., Tayot, X., Plenet, D., Cellier, P., Mchet, J.-M., Meynard, J. M., and Delécolle, R.: STICS: a generic model for the simulation of crops and their water and nitrogen balances. I. Theory and parameterization applied to wheat and corn, *Agronomie*, 18, 311–346, <https://doi.org/10.1051/agro:19980501>, 1998.
- 765 Brown, A. L.: Design Experiments: Theoretical and Methodological Challenges in Creating Complex Interventions in Classroom Settings, *Journal of the Learning Sciences*, 2, 141–178, https://doi.org/10.1207/s15327809jls0202_2, 1992.
- Brus, D. J. and deGrujter, J. J.: Random sampling or geostatistical modelling? Choosing between design-based and model-based sampling strategies for soil (with discussion), *Geoderma*, 80, 1–44, [https://doi.org/10.1016/s0016-7061\(97\)00072-4](https://doi.org/10.1016/s0016-7061(97)00072-4), 1997.

- 775 Brus, D. J. and Saby, N. P. A.: Approximating the variance of estimated means for systematic random sampling, illustrated with data of the French Soil Monitoring Network, *Geoderma*, 279, 77–86, <https://doi.org/10.1016/j.geoderma.2016.05.016>, 2016.
- Buysse, P., Loubet, B., Depuydt, J., Durand, B., and Kalalian, C.: ETC L2 ARCHIVE from Grignon, 2021–2024, <https://hdl.handle.net/11676/PNO4RZY-PWDLIqx2L2HScBMt>, 2025.
- 780 Canty, A., Ripley, B., and Brazzale, A. R.: Package “boot”, <https://doi.org/10.32614/CRAN.package.boot>, 2024.
- Ceschia, E., Béziat, P., Dejoux, J. F., Aubinet, M., Bernhofer, C., Bodson, B., Buchmann, N., Carrara, A., Cellier, P., Di Tommasi, P., Elbers, J. A., Eugster, W., Grünwald, T., Jacobs, C. M. J., Jans, W. W. P., Jones, M., Kutsch, W., Lanigan, G., Magliulo, E., Marloie, O., Moors, E. J., Moureaux, C., Olioso, A., Osborne, B., Sanz, M. J., Saunders, M., Smith, P., Soegaard, H., and Wattenbach, M.: Management effects on net ecosystem carbon and GHG budgets at European crop sites, *Agric Ecosyst Environ*, 139, 363–383, <https://doi.org/10.1016/j.agee.2010.09.020>, 2010.
- 785 Chen, L., Liu, L., Qin, S., Yang, G., Fang, K., Zhu, B., Kuzyakov, Y., Chen, P., Xu, Y., and Yang, Y.: Regulation of priming effect by soil organic matter stability over a broad geographic scale, *Nat Commun*, 10, <https://doi.org/10.1038/s41467-019-13119-z>, 2019.
- 790 Chenu, C., Angers, D. A., Barré, P., Derrien, D., Arrouays, D., and Balesdent, J.: Increasing organic stocks in agricultural soils: Knowledge gaps and potential innovations, *Soil Tillage Res*, 188, 41–52, <https://doi.org/https://doi.org/10.1016/j.still.2018.04.011>, 2019.
- Clivot, H., Mouny, J.-C., Duparque, A., Dinh, J.-L., Denoroy, P., Houot, S., Vertès, F., Trochard, R., Bouthier, A., Sagot, S., and Mary, B.: Modeling soil organic carbon evolution in long-term arable experiments with AMG model, *Environmental Modelling & Software*, 118, 99–113, <https://doi.org/https://doi.org/10.1016/j.envsoft.2019.04.004>, 2019.
- 795 Clivot, H., Duparque, A., Ferchaud, F., Lagrange, H., Levvasseur, F., Levert, M., Marsac, S., Mary, B., Mouny, J.-C., Piquemal, B., Sagot, S., Servain, F., Trochard, R., Cadoux, S., and Perrin, A.-S.: AMGv2 parameters, <https://doi.org/https://doi.org/10.57745/MEQQIX>, 7 June 2023.
- 800 Coleman, K. and Jenkinson, D. S.: RothC-26.3 - A Model for the turnover of carbon in soil, in: *Evaluation of Soil Organic Matter Models*, Springer Berlin Heidelberg, Berlin, Heidelberg, 237–246, https://doi.org/10.1007/978-3-642-61094-3_17, 1996.
- Collins, A.: Toward a Design Science of Education, in: *New Directions in Educational Technology*, edited by: Scanlon, E. and O’Shea, T., Springer Berlin Heidelberg, Berlin, Heidelberg, 15–22, https://doi.org/10.1007/978-3-642-77750-9_2, 1992.
- 805 Corti, G., Ugolini, F. C., and Agnelli, A.: Classing the Soil Skeleton (Greater than Two Millimeters): Proposed Approach and Procedure, *Soil Science Society of America Journal*, 62, 1620–1629, <https://doi.org/https://doi.org/10.2136/sssaj1998.03615995006200060020x>, 1998.
- De Rosa, D., Ballabio, C., Lugato, E., Fasiolo, M., Jones, A., and Panagos, P.: Soil organic carbon stocks in European croplands and grasslands: How much have we lost in the past decade?, *Glob Chang Biol*, 30, <https://doi.org/10.1111/gcb.16992>, 2024.
- 810 Dimassi, B., Mary, B., Wylleman, R., Labreuche, J. Ô., Couture, D., Piraux, F., and Cohan, J. P.: Long-term effect of contrasted tillage and crop management on soil carbon dynamics during 41 years, *Agric Ecosyst Environ*, 188, 134–146, <https://doi.org/10.1016/j.agee.2014.02.014>, 2014.
- 815 Don, A., Schumacher, J., Scherer-Lorenzen, M., Scholten, T., and Schulze, E.-D.: Spatial and vertical variation of soil carbon at two grassland sites — Implications for measuring soil carbon stocks, *Geoderma*, 141, 272–282, <https://doi.org/https://doi.org/10.1016/j.geoderma.2007.06.003>, 2007.
- Du, Z., Angers, D. A., Ren, T., Zhang, Q., and Li, G.: The effect of no-till on organic C storage in Chinese soils should not be overemphasized: A meta-analysis, *Agric Ecosyst Environ*, 236, 1–11, <https://doi.org/https://doi.org/10.1016/j.agee.2016.11.007>, 2017.
- 820 Efron, B.: Better Bootstrap Confidence Intervals, *J Am Stat Assoc*, 82, 171–185, <https://doi.org/10.1080/01621459.1987.10478410>, 1987.
- Ellert, B. H. and Bettany, J. R.: Calculation of organic matter and nutrients stored in soils under contrasting management regimes, *Can J Soil Sci*, 75, 529–538, <https://doi.org/10.4141/cjss95-075>, 1995.
- 825 Fan, J., McConkey, B., Wang, H., and Janzen, H.: Root distribution by depth for temperate agricultural crops, *Field Crops Res*, 189, 68–74, <https://doi.org/10.1016/j.fcr.2016.02.013>, 2016.
- FAO: Measuring and modelling soil carbon stocks and stock changes in livestock production systems: Guidelines for assessment, Versuib 1., *Livestock Environmental Assessment and Performance (LEAP) Partnership*, Rome, 170 pp., 2019.
- 830 Ferchaud, F., Chlebowski, F., and Mary, B.: SimpleESM: R script to calculate soil organic carbon and nitrogen stocks at Equivalent Soil Mass, 1–9 pp., 2023.
- Franzluebbers, A. J., Paine, L. K., Winsten, J. R., Krome, M., Sanderson, M. A., Ogles, K., and Thompson, D.: Well-managed grazing systems: A forgotten hero of conservation, *J Soil Water Conserv*, 67, <https://doi.org/10.2489/jswc.67.4.100A>, 2012.

- 835 Goovaerts, P.: Geostatistics for natural resources evaluation, Oxford University Press, New York, 0–483 pp.,
<https://doi.org/https://doi.org/10.1023/A:1007530422454>, 1997.
- Gräler, B., Pebesma, E., and Heuvelink, G.: Spatio-Temporal Interpolation using gstat, *R J*, 8, 204,
<https://doi.org/10.32614/RJ-2016-014>, 2016.
- de Gruijter, J. J., Bierkens, M. F. P., Brus, D. J., and Knotters, M.: Sampling for Natural Resource Monitoring,
 Springer Berlin Heidelberg, Berlin, Heidelberg, 334 pp., <https://doi.org/10.1007/3-540-33161-1>, 2006.
- 840 von Haden, A. C., Yang, W. H., and DeLucia, E. H.: Soils’ dirty little secret: Depth-based comparisons can be
 inadequate for quantifying changes in soil organic carbon and other mineral soil properties, *Glob Chang
 Biol*, 26, 3759–3770, <https://doi.org/10.1111/gcb.15124>, 2020.
- Hamza, M. A. and Anderson, W. K.: Soil compaction in cropping systems, *Soil Tillage Res*, 82, 121–145,
<https://doi.org/10.1016/j.still.2004.08.009>, 2005.
- 845 Harbo, L. S., Olesen, J. E., Liang, Z., Christensen, B. T., and Elsgaard, L.: Estimating organic carbon stocks of
 mineral soils in Denmark: Impact of bulk density and content of rock fragments, *Geoderma Regional*, 30,
 e00560, <https://doi.org/https://doi.org/10.1016/j.geodrs.2022.e00560>, 2022.
- Hedges, L. V.: Distribution theory for Glass’s estimator of effect size and related estimators, *Journal of Educational
 Statistics*, 6, 107–128, <https://doi.org/10.2307/1164588>, 1981.
- 850 Heiskanen, J., Brummer, C., Buchmann, N., Calfapietra, C., Chen, H., Gielen, B., Gkritzalis, T., Hammer, S.,
 Hartman, S., Herbst, M., Janssens, I. A., Jordan, A., Juurola, E., Karstens, U., Kasurinen, V., Kruijt, B.,
 Lankreijer, H., Levin, I., Linderson, M. L., Loustau, D., Merbold, L., Myhre, C. L., Papale, D., Pavelka,
 M., Pilegaard, K., Ramonet, M., Rebmann, C., Rinne, J., Rivier, L., Saltikoff, E., Sanders, R., Steinbacher,
 M., Steinhoff, T., Watson, A., Vermeulen, A. T., Vesala, T., Vítková, G., and Kutsch, W.: The Integrated
 855 Carbon Observation System in Europe, *Bull Am Meteorol Soc*, 103, E855–E872,
<https://doi.org/10.1175/BAMS-D-19-0364.1>, 2022.
- Hijmans, R. J.: raster: Geographic Data Analysis and Modeling, <https://doi.org/10.32614/CRAN.package.raster>,
 20 March 2010.
- 860 Hopkins, D. W., Waite, I. S., McNicol, J. W., Poulton, P. R., Macdonald, A. J., and O’Donnell, A. G.: Soil organic
 carbon contents in long-term experimental grassland plots in the UK (Palace Leas and Park Grass) have not
 changed consistently in recent decades, *Glob Chang Biol*, 15, 1739–1754, [https://doi.org/10.1111/j.1365-
 2486.2008.01809.x](https://doi.org/10.1111/j.1365-

 2486.2008.01809.x), 2009.
- Ingwersen, J., Poyda, A., Kremer, P., and Streck, T.: Harvest residues: A relevant term in the carbon balance of
 croplands?, *Agric For Meteorol*, 349, <https://doi.org/10.1016/j.agrformet.2024.109935>, 2024.
- 865 IPCC: Generic methodologies applicable to multiple land-use categories, Refinement to the 2006 IPCC guidelines,
 2019.
- Kanari, E., Cécillon, L., Baudin, F., Clivot, H., Ferchaud, F., Houot, S., Levvasseur, F., Mary, B., Soucémari-
 nadin, L., Chenu, C., and Barré, P.: A robust initialization method for accurate soil organic carbon simula-
 tions, *Biogeosciences*, 19, 375–387, <https://doi.org/10.5194/bg-19-375-2022>, 2022.
- 870 Keel, S. G., Anken, T., Büchi, L., Chervet, A., Fliessbach, A., Flisch, R., Huguenin-Elie, O., Mäder, P., Mayer, J.,
 Sinaj, S., Sturny, W., Wüst-Galley, C., Zihlmann, U., and Leifeld, J.: Loss of soil organic carbon in Swiss
 long-term agricultural experiments over a wide range of management practices, *Agric Ecosyst Environ*,
 286, <https://doi.org/10.1016/j.agee.2019.106654>, 2019.
- Keel, S. G., Budai, A., Elsgaard, L., Hardy, B., Levvasseur, F., Zhi, L., Mondini, C., Plaza, C., and Leifeld, J.:
 875 Efficiency of Plant Biomass Processing Pathways for Long-Term Soil Carbon Storage, *Eur J Soil Sci*, 76,
<https://doi.org/10.1111/ejss.70074>, 2025.
- Kindler, R., Siemens, J., Kaiser, K., Walmsley, D. C., Bernhofer, C., Buchmann, N., Cellier, P., Eugster, W.,
 Gleixner, G., Grunwald, T., Heim, A., Ibrom, A., Jones, S. K., Jones, M., Klumpp, K., Kutsch, W., Larsen,
 K. S., Lehuger, S., Loubet, B., McKenzie, R., Moors, E., Osborne, B., Pilegaard, K., Rebmann, C., Saun-
 880 ders, M., Schmidt, M. W. I., Schrupf, M., Seyfferth, J., Skiba, U., Soussana, J. F., Sutton, M. A., Tefs,
 C., Vowinkel, B., Zeeman, M. J., and Kaupenjohann, M.: Dissolved carbon leaching from soil is a crucial
 component of the net ecosystem carbon balance, *Glob Chang Biol*, 17, 1167–1185,
<https://doi.org/10.1111/j.1365-2486.2010.02282.x>, 2011.
- Kirby, K. N. and Gerlanc, D.: BootES: An R package for bootstrap confidence intervals on effect sizes, *Behav Res
 885 Methods*, 45, 905–927, <https://doi.org/10.3758/s13428-013-0330-5>, 2013.
- Kleber, M., Bourg, I. C., Coward, E. K., Hansel, C. M., Myneni, S. C. B., and Nunan, N.: Dynamic interactions at
 the mineral–organic matter interface, <https://doi.org/10.1038/s43017-021-00162-y>, 11 May 2021.
- Kljun, N., Calanca, P., Rotach, M. W., and Schmid, H. P.: A Simple Parameterisation for Flux Footprint Predic-
 tions, *Boundary Layer Meteorol*, 112, 503–523, <https://doi.org/10.1023/B:BOUN.0000030653.71031.96>,
 890 2004.
- Kljun, N., Calanca, P., Rotach, M. W., and Schmid, H. P.: A simple two-dimensional parameterisation for Flux
 Footprint Prediction (FFP), *Geosci. Model Dev.*, 8, 3695–3713, <https://doi.org/10.5194/gmd-8-3695-2015>,
 2015.

- 895 Knotters, M., Teuling, K., Reijneveld, A., Lesschen, J. P., and Kuikman, P.: Changes in organic matter contents and carbon stocks in Dutch soils, 1998–2018, *Geoderma*, 414, <https://doi.org/10.1016/j.geoderma.2022.115751>, 2022.
- Krauss, M., Wiesmeier, M., Don, A., Cuperus, F., Gattinger, A., Gruber, S., Haagsma, W. K., Peigné, J., Palazzoli, M. C., Schulz, F., van der Heijden, M. G. A., Vincent-Caboud, L., Wittwer, R. A., Zikeli, S., and Steffens, M.: Reduced tillage in organic farming affects soil organic carbon stocks in temperate Europe, *Soil Tillage Res*, 216, <https://doi.org/10.1016/j.still.2021.105262>, 2022.
- 900 Lal, R.: Carbon emission from farm operations, *Environ Int*, 30, 981–990, <https://doi.org/10.1016/j.envint.2004.03.005>, 2004.
- Launay, C., Constantin, J., Chlebowski, F., Houot, S., Graux, A. I., Klumpp, K., Martin, R., Mary, B., Pellerin, S., and Therond, O.: Estimating the carbon storage potential and greenhouse gas emissions of French arable cropland using high-resolution modeling, *Glob Chang Biol*, 27, 1645–1661, <https://doi.org/10.1111/gcb.15512>, 2021.
- 905 Lee, J., Hopmans, J. W., Rolston, D. E., Baer, S. G., and Six, J.: Determining soil carbon stock changes: Simple bulk density corrections fail, *Agric Ecosyst Environ*, 134, 251–256, <https://doi.org/10.1016/j.agee.2009.07.006>, 2009.
- 910 Liebhard, G., Toth, M., Stumpp, C., Bodner, G., Klik, A., Zhang, X., Strohmeier, S., and Strauss, P.: Developing topsoil structure through conservation management to protect subsoil from compaction, *Soil Tillage Res*, 253, 106669, <https://doi.org/10.1016/j.still.2025.106669>, 2025.
- Lipiec, J. and Hatano, R.: Quantification of compaction effects on soil physical properties and crop growth, *Geoderma*, 116, 107–136, [https://doi.org/10.1016/S0016-7061\(03\)00097-1](https://doi.org/10.1016/S0016-7061(03)00097-1), 2003.
- 915 Liu, J., Wu, P., Zhao, Z., and Gao, Y.: Afforestation on cropland promotes pedogenic inorganic carbon accumulation in deep soil layers on the Chinese loess plateau, *Plant Soil*, 478, 597–612, <https://doi.org/10.1007/s11104-022-05494-2>, 2022.
- Loubet, B., Laville, P., Lehuger, S., Larmanou, E., Fléchar, C., Mascher, N., Genermont, S., Roche, R., Ferrara, R. M., Stella, P., Personne, E., Durand, B., Decuq, C., Flura, D., Masson, S., Fanucci, O., Rampon, J. N., Siemens, J., Kindler, R., Gabrielle, B., Schrupf, M., and Cellier, P.: Carbon, nitrogen and Greenhouse gases budgets over a four years crop rotation in northern France, *Plant Soil*, 343, 109–137, <https://doi.org/10.1007/s11104-011-0751-9>, 2011.
- 920 Loustau, D., Jolivet, C., Lafont, S., Loubet, B., Klumpp, K., Papale, D., and Arrouays, D.: ICOS Ecosystem Instructions for Soil Samples Collection and Preparation (Version 20230727), <https://doi.org/https://doi.org/10.18160/k3yc-td6h>, 2017.
- 925 Lu, H., Li, S., Ma, M., Bastrikov, V., Chen, X., Ciais, P., Dai, Y., Ito, A., Ju, W., Lienert, S., Lombardozzi, D., Lu, X., Maignan, F., Nakhavali, M., Quine, T., Schindlbacher, A., Wang, J., Wang, Y., Wrlind, D., Zhang, S., and Yuan, W.: Comparing machine learning-derived global estimates of soil respiration and its components with those from terrestrial ecosystem models, *Environmental Research Letters*, 16, <https://doi.org/10.1088/1748-9326/abf526>, 2021.
- 930 MacQueen, J.: Some methods for classification and analysis of multivariate observations, in: *Proceedings of the Fifth Berkeley Symposium on Mathematical Statistics and Probability*, 666, 1967.
- Mary, B., Clivot, H., Blaszczyk, N., Labreuche, J., and Ferchaud, F.: Soil carbon storage and mineralization rates are affected by carbon inputs rather than physical disturbance: Evidence from a 47-year tillage experiment, *Agric Ecosyst Environ*, 299, <https://doi.org/10.1016/j.agee.2020.106972>, 2020.
- 935 McBratney, Alex. B. and Minasny, B.: Comment on “Determining soil carbon stock changes: Simple bulk density corrections fail” [*Agric. Ecosyst. Environ.* 134 (2009) 251–256], *Agric Ecosyst Environ*, 136, 185–186, <https://doi.org/10.1016/j.agee.2009.12.010>, 2010.
- 940 Meersmans, J., Arrouays, D., Van Rompaey, A. J. J., Pagé, C., De Baets, S., and Quine, T. A.: Future C loss in mid-latitude mineral soils: Climate change exceeds land use mitigation potential in France, *Sci Rep*, 6, <https://doi.org/10.1038/srep35798>, 2016.
- 945 Minasny, B., Malone, B. P., McBratney, A. B., Angers, D. A., Arrouays, D., Chambers, A., Chaplot, V., Chen, Z.-S., Cheng, K., Das, B. S., Field, D. J., Gimona, A., Hedley, C. B., Hong, S. Y., Mandal, B., Marchant, B. P., Martin, M., McConkey, B. G., Mulder, V. L., O’Rourke, S., Richer-de-Forges, A. C., Odeh, I., Padarian, J., Paustian, K., Pan, G., Poggio, L., Savin, I., Stolbovoy, V., Stockmann, U., Sulaeman, Y., Tsui, C.-C., Vågen, T.-G., van Wesemael, B., and Winowiecki, L.: Soil carbon 4 per mille, *Geoderma*, 292, 59–86, <https://doi.org/https://doi.org/10.1016/j.geoderma.2017.01.002>, 2017.
- Molteni, F. and Corti, S.: Long-term fluctuations in the statistical properties of low-frequency variability: dynamical origin and predictability, *Quarterly Journal of the Royal Meteorological Society*, 124, 495–526, 1998.
- 950 Parton, W. J., Hartman, M., Ojima, D., and Schimel, D.: DAYCENT and its land surface submodel: description and testing, *Glob Planet Change*, 19, 35–48, [https://doi.org/10.1016/S0921-8181\(98\)00040-X](https://doi.org/10.1016/S0921-8181(98)00040-X), 1998.
- Paustian, K., Lehmann, J., Ogle, S., Reay, D., Robertson, G. P., and Smith, P.: Climate-smart soils, <https://doi.org/10.1038/nature17174>, 6 April 2016.

- 955 Pebesma, E.: Simple Features for R: Standardized Support for Spatial Vector Data, *R J*, 10, 439, <https://doi.org/10.32614/RJ-2018-009>, 2018.
- Pebesma, E. and Bivand, R.: *Spatial Data Science*, Chapman and Hall/CRC, New York, <https://doi.org/10.1201/9780429459016>, 2023.
- Pebesma, E. J.: Multivariable geostatistics in S: the gstat package, *Comput Geosci*, 30, 683–691, <https://doi.org/10.1016/j.cageo.2004.03.012>, 2004.
- 960 Peng, Y., Chahal, I., Hooker, D. C., and Van Eerd, L. L.: Comparison of equivalent soil mass approaches to estimate soil organic carbon stocks under long-term tillage, *Soil Tillage Res*, 238, <https://doi.org/10.1016/j.still.2024.106021>, 2024.
- Petrescu, A. M. R., McGrath, M. J., Andrew, R. M., Peylin, P., Peters, G. P., Ciais, P., Broquet, G., Tubiello, F. N., Gerbig, C., Pongratz, J., Janssens-Maenhout, G., Grassi, G., Nabuurs, G. J., Regnier, P., Lauerwald, R., Kuhnert, M., Balkovič, J., Schelhaas, M. J., van der Gon, H. A. C. D., Solazzo, E., Qiu, C., Pilli, R., Kononov, I. B., Houghton, R. A., Günther, D., Perugini, L., Crippa, M., Ganzenmüller, R., Luijkx, I. T., Smith, P., Munassar, S., Thompson, R. L., Conchedda, G., Monteil, G., Scholze, M., Karstens, U., Brockmann, P., and Dolman, A. J.: The consolidated European synthesis of CO₂ emissions and removals for the European Union and United Kingdom: 1990–2018, <https://doi.org/10.5194/essd-13-2363-2021>, 28 May 2021.
- 970 Poeplau, C. and Don, A.: Carbon sequestration in agricultural soils via cultivation of cover crops - A meta-analysis, *Agric Ecosyst Environ*, 200, 33–41, <https://doi.org/10.1016/j.agee.2014.10.024>, 2015.
- Poeplau, C., Vos, C., and Don, A.: Soil organic carbon stocks are systematically overestimated by misuse of the parameters bulk density and rock fragment content, *SOIL*, 3, 61–66, <https://doi.org/10.5194/soil-3-61-2017>, 2017.
- 975 Poyda, A., Wizemann, H.-D., Ingwersen, J., Eshonkulov, R., Högy, P., Demyan, M. S., Kremer, P., Wulfmeyer, V., and Streck, T.: Carbon fluxes and budgets of intensive crop rotations in two regional climates of south-west Germany, *Agric Ecosyst Environ*, 276, 31–46, <https://doi.org/10.1016/j.agee.2019.02.011>, 2019.
- R Core Team: A language and environment for statistical computing, <https://www.R-project.org/>, 2025.
- 980 Raza, S., Miao, N., Wang, P. Z., Ju, X. T., Chen, Z. J., Zhou, J. B., and Kuzyakov, Y.: Dramatic loss of inorganic carbon by nitrogen-induced soil acidification in Chinese croplands, *Glob Chang Biol*, 26, 3738–3751, <https://doi.org/10.1111/gcb.15101>, 2020.
- Raza, S., Zamanian, K., Ullah, S., Kuzyakov, Y., Virto II, and Zhou, J. B.: Inorganic carbon losses by soil acidification jeopardize global efforts on carbon sequestration and climate change mitigation, *J Clean Prod*, 315, <https://doi.org/10.1016/j.jelepro.2021.128036>, 2021.
- 985 Rovira, P., Sauras, T., Salgado, J., and Merino, A.: Towards sound comparisons of soil carbon stocks: A proposal based on the cumulative coordinates approach, *Catena (Amst)*, 133, 420–431, <https://doi.org/10.1016/j.catena.2015.05.020>, 2015.
- Rumpel, C. and Kögel-Knabner, I.: Deep soil organic matter—a key but poorly understood component of terrestrial C cycle, *Plant Soil*, 338, 143–158, <https://doi.org/10.1007/s11104-010-0391-5>, 2011.
- 990 Saby, N. P. A., Bellamy, P. H., Morvan, X., Arrouays, D., Jones, R. J. A., Verheijen, F. G. A., Kibblewhite, M. G., Verdoodt, A., Berenyiueves, J., Freudenschuss, A., and Simota, C.: Will European soil-monitoring networks be able to detect changes in topsoil organic carbon content?, *Glob Chang Biol*, 14, 2432–2442, <https://doi.org/10.1111/j.1365-2486.2008.01658.x>, 2008.
- 995 Sanderman, J., Hengl, T., and Fiske, G. J.: Soil carbon debt of 12,000 years of human land use, *Proceedings of the National Academy of Sciences*, 114, 9575–9580, <https://doi.org/doi:10.1073/pnas.1706103114>, 2017.
- Schimel, D. S.: Terrestrial ecosystems and the carbon cycle, *Glob Chang Biol*, 1, 77–91, <https://doi.org/10.1111/j.1365-2486.1995.tb00008.x>, 1995.
- 1000 Schmidt, M. W. I., Torn, M. S., Abiven, S., Dittmar, T., Guggenberger, G., Janssens, I. A., Kleber, M., Kögel-Knabner, I., Lehmann, J., Manning, D. A. C., Nannipieri, P., Rasse, D. P., Weiner, S., and Trumbore, S. E.: Persistence of soil organic matter as an ecosystem property, <https://doi.org/10.1038/nature10386>, 6 October 2011.
- Schrumpf, M., Schulze, E. D., Kaiser, K., and Schumacher, J.: How accurately can soil organic carbon stocks and stock changes be quantified by soil inventories?, *Biogeosciences*, 8, 1193–1212, <https://doi.org/10.5194/bg-8-1193-2011>, 2011.
- 1005 Schulze, E. D., Luysaert, S., Ciais, P., Freibauer, A., Janssens, I. A., Soussana, J. F., Smith, P., Grace, J., Levin, I., Thiruchittampalam, B., Heimann, M., Dolman, A. J., Valentini, R., Bousquet, P., Peylin, P., Peters, W., Rödenbeck, C., Etiope, G., Vuichard, N., Wattenbach, M., Nabuurs, G. J., Poussi, Z., Nieschulze, J., and Gash, J. H.: Importance of methane and nitrous oxide for Europe’s terrestrial greenhouse-gas balance, *Nat Geosci*, 2, 842–850, <https://doi.org/10.1038/ngeo686>, 2009.
- 1010 Shepard, D.: A two-dimensional interpolation function for irregularly-spaced data, in: *Proceedings of the 1968 23rd ACM national conference on* -, 517–524, <https://doi.org/10.1145/800186.810616>, 1968.

- Six, J., Conant, R. T., Paul, E. A., and Paustian, K.: Stabilization mechanisms of soil organic matter: Implications for C-saturation of soils, *Plant and Soil*, 155–176 pp., 2002.
- 1015 Skadell, L. E., Schneider, F., Gocke, M. I., Guigue, J., Amelung, W., Bauke, S. L., Hobbey, E. U., Barkusky, D., Honermeier, B., Kögel-Knabner, I., Schmidhalter, U., Schweitzer, K., Seidel, S. J., Siebert, S., Sommer, M., Vaziritarbar, Y., and Don, A.: Twenty percent of agricultural management effects on organic carbon stocks occur in subsoils – Results of ten long-term experiments, *Agric Ecosyst Environ*, 356, <https://doi.org/10.1016/j.agee.2023.108619>, 2023.
- 1020 Soleilhavoup, M. and Crisan, M.: Enquête pratiques culturales en grandes cultures et prairies 2017 - Principaux résultats (Version modifiée), <https://agreste.agriculture.gouv.fr/agreste-web/disaron/Chd2009/detail/>, 2021.
- Song, X. D., Yang, F., Wu, H. Y., Zhang, J., Li, D. C., Liu, F., Zhao, Y. G., Yang, J. L., Ju, B., Cai, C. F., Huang, B. A., Long, H. Y., Lu, Y., Sui, Y. Y., Wang, Q. B., Wu, K. N., Zhang, F. R., Zhang, M. K., Shi, Z., Ma, W. Z., Xin, G., Qi, Z. P., Chang, Q. R., Ci, E., Yuan, D. G., Zhang, Y. Z., Bai, J. P., Chen, J. Y., Chen, J., Chen, Y. J., Dong, Y. Z., Han, C. L., Li, L., Liu, L. M., Pan, J. J., Song, F. P., Sun, F. J., Wang, D. F., Wang, T. W., Wei, X. H., Wu, H. Q., Zhao, X., Zhou, Q., and Zhang, G. L.: Significant loss of soil inorganic carbon on the continental scale, *Natl Sci Rev*, 9, <https://doi.org/10.1093/nsr/nwab120>, 2022.
- 1030 Tardieu, F.: Analysis of the spatial variability of maize root density .1. Effect of wheel compaction on the spatial arrangement of roots, *Plant Soil*, 107, 259–266, <https://doi.org/10.1007/bf02370555>, 1988.
- Tennekes, M.: tmap: Thematic maps in R, *J Stat Softw*, 84, <https://doi.org/10.18637/jss.v084.i06>, 2018.
- Thomsen, I. K., Olesen, J. E., Møller, H. B., Sørensen, P., and Christensen, B. T.: Carbon dynamics and retention in soil after anaerobic digestion of dairy cattle feed and faeces, *Soil Biol Biochem*, 58, 82–87, <https://doi.org/10.1016/j.soilbio.2012.11.006>, 2013.
- 1035 Thorndike, R. L.: Who Belongs in the Family?, *Psychometrika*, 18, 267–276, <https://doi.org/10.1007/BF02289263>, 1953.
- Tian, H., Pan, N., Thompson, R. L., Canadell, J. G., Suntharalingam, P., Regnier, P., Davidson, E. A., Prather, M., Ciais, P., Muntean, M., Pan, S., Winiwarter, W., Zaehle, S., Zhou, F., Jackson, R. B., Bange, H. W., Berthet, S., Bian, Z., Bianchi, D., Bouwman, A. F., Buitenhuis, E. T., Dutton, G., Hu, M., Ito, A., Jain, A. K., Jeltsch-Thömmes, A., Joos, F., Kou-Giesbrecht, S., Krummel, P. B., Lan, X., Landolfi, A., Lauerwald, R., Li, Y., Lu, C., Maavara, T., Manizza, M., Millet, D. B., Mühle, J., Patra, P. K., Peters, G. P., Qin, X., Raymond, P., Resplandy, L., Rosentreter, J. A., Shi, H., Sun, Q., Tonina, D., Tubiello, F. N., van der Werf, G. R., Vuichard, N., Wang, J., Wells, K. C., Western, L. M., Wilson, C., Yang, J., Yao, Y., You, Y., and Zhu, Q.: Global nitrous oxide budget (1980–2020), *Earth Syst Sci Data*, 16, 2543–2604, <https://doi.org/10.5194/essd-16-2543-2024>, 2024.
- 1040 VandenBygaart, A. J. and Angers, D. A.: Towards accurate measurements of soil organic carbon stock change in agroecosystems, *Can J Soil Sci*, 86, 465–471, <https://doi.org/10.4141/s05-106>, 2006.
- 1050 Walvoort, D. J. J., Brus, D. J., and de Gruijter, J. J.: An R package for spatial coverage sampling and random sampling from compact geographical strata by k-means, *Comput Geosci*, 36, 1261–1267, <https://doi.org/https://doi.org/10.1016/j.cageo.2010.04.005>, 2010.
- Wendt, J. W. and Hauser, S.: An equivalent soil mass procedure for monitoring soil organic carbon in multiple soil layers, *Eur J Soil Sci*, 64, 58–65, <https://doi.org/10.1111/ejss.12002>, 2013.
- 1055 Wiesmeier, M., Sporlein, P., Geuss, U., Hangen, E., Haug, S., Reischl, A., Schilling, B., von Lutzow, M., and Kögel-Knabner, I.: Soil organic carbon stocks in southeast Germany (Bavaria) as affected by land use, soil type and sampling depth, *Glob Chang Biol*, 18, 2233–2245, <https://doi.org/10.1111/j.1365-2486.2012.02699.x>, 2012.
- Xiao, L., Zhou, S., Zhao, R., Greenwood, P., and Kuhn, N. J.: Evaluating soil organic carbon stock changes induced by no-tillage based on fixed depth and equivalent soil mass approaches, *Agric Ecosyst Environ*, 300, 106982, <https://doi.org/10.1016/j.agee.2020.106982>, 2020.
- 1060 Xu, L., He, N. P., Yu, G. R., Wen, D., Gao, Y., and He, H. L.: Differences in pedotransfer functions of bulk density lead to high uncertainty in soil organic carbon estimation at regional scales: Evidence from Chinese terrestrial ecosystems, *J Geophys Res Biogeosci*, 120, 1567–1575, <https://doi.org/10.1002/2015JG002929>, 2015.
- Zamanian, K., Zhou, J. B., and Kuzyakov, Y.: Soil carbonates: The unaccounted, irrecoverable carbon source, *Geoderma*, 384, <https://doi.org/10.1016/j.geoderma.2020.114817>, 2021.
- 1065 Zhang, B., Jia, Y., Fan, H., Guo, C., Fu, J., Li, S., Li, M., Liu, B., and Ma, R.: Soil compaction due to agricultural machinery impact: A systematic review, *Land Degrad Dev*, 35, 3256–3273, <https://doi.org/10.1002/ldr.5144>, 2024.
- Zhang, X. X., Whalley, P. A., Ashton, R. W., Evans, J., Hawkesford, M. J., Griffiths, S., Huang, Z. D., Zhou, H., Mooney, S. J., and Whalley, W. R.: A comparison between water uptake and root length density in winter wheat: effects of root density and rhizosphere properties, *Plant Soil*, 451, 345–356, <https://doi.org/10.1007/s11104-020-04530-3>, 2020.
- 1070

Zou, J., Ziegler, A. D., Chen, D., McNicol, G., Ciais, P., Jiang, X., Zheng, C., Wu, J., Wu, J., Lin, Z., He, X., Brown, L. E., Holden, J., Zhang, Z., Ramchunder, S. J., Chen, A., and Zeng, Z.: Rewetting global wetlands effectively reduces major greenhouse gas emissions, *Nat Geosci*, 15, 627–632, <https://doi.org/10.1038/s41561-022-00989-0>, 2022.

1075